Lung Tissue Engineering: *In Vitro* Synthesis of Lung Tissue from Neonatal and Fetal Rat Lung Cells Cultured in a Three-Dimensional Collagen Matrix

by

Patty P. Chen

Submitted in Partial Fulfillment of the Requirements for the Degree of Master of Engineering in Biomedical Engineering in the Harvard-MIT Division of Health Science and Technology at the Massachusetts Institute of Technology in August 2004 [September]

Author _____ 8/4/04
Department of Health Science & Technology
Date, 2004

Certified by _____
Myron Spector
Thesis Supervisor

Certified by _____
Ioannis V. Yannas
Thesis Co-Supervisor

Accepted by _____
Roger Mark
Chairman, Department Committee on Graduate Thesis

Accepted by: _____
Martha L. Gray, Ph.D.
Edward Hood Taplin Professor of Medical and Electrical Engineering
Co-Director, Harvard-MIT Division of Health Sciences and Technology

Lung Tissue Engineering: *In Vitro* Synthesis of Lung Tissue from Neonatal and Fetal Rat Lung Cells Cultured in a Three-Dimensional Collagen Matrix

by

Patty P. Chen

Submitted to the
Department of Health Science & Technology

August 6, 2004

In Partial Fulfillment of the Requirements for the Degree of
Master of Engineering in Biomedical Engineering

ABSTRACT

The focus of this study was to investigate the histology of tissue formed when fetal (16-20 days gestation) and neonatal (2 days old) rat lung cells were grown in a collagen-glycosaminoglycan scaffold. This project employed a collagen-GAG scaffold specifically developed for tissue engineering and investigated the effect of this substratum on the formation of lung histotypic structures *in vitro*. A cell isolation procedure was developed whereby 19-days gestation type II alveolar cells reaggregated to form alveolar-like structures. The effects of selected scaffold design variables including pore diameter and degradation rate of the substratum on lung tissue regeneration were explored. Lung cell behavior revealed as the cells interact with an analog of the extracellular matrix was also examined. Differences in fetal and neonatal lung cell behavior were identified using histological analysis. Lung cells were obtained from Sprague-Dawley rats after 16-, 19-, and 20-days of gestation and at 2 days after term. These cells were seeded into type I collagen-GAG matrices, sized 8mm in diameter by 2mm in thickness. The medium used, F12K and Ham's nutrient mixture, was supplemented with 10% fetal bovine serum. A seeding density between 1 to 5 million cells per sponge sample was used. Histology studies were performed at termination periods of 2, 14, and 28 days. This paper describes the *in vitro* formation and long-term maintenance of alveolar-like structures from enzymatically dissociated 19-days gestation fetal rat lung cells cultured on a collagen sponge substrate as a model system for lung tissue engineering.

Thesis Supervisor: Myron Spector, Ph.D
Title: Professor of Orthopaedic Surgery (Biomaterials), Harvard Medical School
Thesis Co-Supervisor: Ioannis V. Yannas, Ph.D
Title: Professor of Mechanical Engineering, Massachusetts Institute of Technology

Acknowledgements

I would like to thank Dr. Myron Spector who has been my supervisor, professor, and advisor. I have been truly fortunate to work with a man who is always so optimistic and supportive of all my endeavors.

I would also like to thank Dr. Ioannis Yannas who has been my engineering supervisor for this thesis and his Polymer Lab for the collagen-GAG scaffolds used in the studies. Thanks to Brandon Harley who taught me how to fabricate the matrices.

I am very grateful to Dr. Erika Marsilio for being there every step of the way and helping me set everything up. I am also very grateful to Camille Francois for all his work and help with the many samples that needed to be processed and stained for histology studies.

From Boston University, I would like to thank Ed Lucey for his generosity and for providing the mice cells and Rossie Clark-Cotton for teaching me how to perform the cell isolation procedure.

At the VA Animal Facility, thanks to Diane and Alex Ghera for being very helpful in setting up an area for the rats.

Thanks to everyone in our lab for their help in many ways throughout my time at the VA Research facility. In particular, thanks to Ramille Capito, Tim Gordon, Leonide Saad, Scott Vickers, Sajjad Matin for their friendship and help.

Lastly, I would like to dedicate this thesis to my family – Jim, Monica, Kathy, and Carlene Chen. Thanks for always supporting me from the beginning to the end.

Table of Contents

List of Figures

List of Tables

Chapter 1 Introduction and Background

1.1 Purpose of Research

The incidence of lung disease has risen steadily due to the increase in cigarette smoking, air pollution, and other environmental inhalants. Destructive lung diseases such as cystic fibrosis, primary pulmonary disease, idiopathic pulmonary fibrosis, and chronic obstructive pulmonary disease ultimately require lung transplantation. In patients with lung impairment and limited life expectancy, successful transplantation can significantly improve their quality of life and prolong survival. About 18 to 20 million people suffer from chronic obstructive pulmonary disease (COPD) including chronic bronchitis. It is estimated that 1.6 to 3 million people suffer from emphysema alone, 50,000 people suffer from idiopathic pulmonary fibrosis, and the same number from cystic fibrosis in the US [1]. However, due to a fixed pool of lung donors in the midst of a growing patient population in need of transplantation, about 3:1 transplants needed are provided, so the waiting period could be more than two years. The result is a stagnant annual lung transplantation rate and an increase in the number of people who die waiting [2]. In the US, only about 1,200 lung transplants are performed annually. Despite today's medical and surgical advances, lung transplantation outcomes still remain poor with a median survival time of five years [3]. Reasons for its limited success are due to immune-mediated allograft rejection and secondary complications from immunosuppressive therapy. It is clear that research and scientific and clinical advances in lung tissue engineering are greatly needed.

New insights into lung tissue engineering can emerge from an improved understanding of lung structural development and growth. Since early developmental events may be determinative of lung sequel later in life, information on fetal and neonatal lung cell behavior is important. Relatively few cell types play a pivotal role in the development and maintenance of the normal architecture of the lung so insight into cell-cell and cell-matrix interactions could provide important information on how the architecture of the lung is determined.

1.2 Background

1.2.1 Respiratory system

The main function of the respiratory system is to bring oxygen from the atmosphere to the blood so that oxygen-rich arterial blood can perfuse organs in the body and to transport carbon dioxide waste from the tissue to the atmosphere. The system is divisible into three major parts: ventilation, conduction, and respiration. Ventilation creates pressure differences that move air into (inspiration) and out of (expiration) the lungs. The main function of the upper portion of the respiratory system, which includes the pharynx to the terminal bronchioles, is conduction. This portion warms and humidifies the air to enhance gas exchange, carries air to and from the site of gas exchange without collapsing under the pressures generated by the ventilating mechanism, and also removes particulate matter and micro-organisms.

The lower portion of the respiratory system is specialized for respiration. The respiratory portion of the lung is distinguished by the presence of alveoli. The actual site of gas exchange occurs at the alveoli sacs which are composed of clusters of alveoli at the end of the bronchial tree. Alveolar sacs are comprised of thin alveolar walls consisting primarily of a central capillary, bounded on each side by simple squamous epithelium. They are small sacs, approximately 200μm in diameter, which open into respiratory bronchioles, alveolar ducts, and alveolar sacs. Alveoli are separated from each other by thin fenestrated walls called interalveolar septae. The fenestrations, called pores of Kohn, help equilibrate pressures and allow collateral ventilation in the event of a blocked alveolus. Interstitial connective tissues are also present within the septae. The connective tissues include: elastic and collagen fibers, ground substance, fibroblasts, mast cells, macrophages, lymphocytes, and contractile cells which respond to epinephrine and histamine. The blood-air barrier comprises of the structures that oxygen and carbon dioxide must cross in the process of gas exchange. In normal lung tissues, it varies from 0.1 – 1.5μm in thickness and includes 1) a film of pulmonary surfactant of the alveolar surface 2) cytoplasm of the type I epithelial cell 3) the fused basal lamina between the type I epithelial cells and endothelial cells of the capillary 4) cytoplasm of the capillary

endothelial cell 5) plasma of the circulating blood and 6) the erythrocyte plasma membrane.[4]

1.2.2 Lung anatomy

The trachea bifurcates into two main bronchi which enter the right and left lung (**Figure 1**). The right lung is divided into three lobes: upper, middle, lower. The left lung only has two lobes: upper and lower. The upper left lobe includes the lingual which is homologous to the middle right lobe. [5]

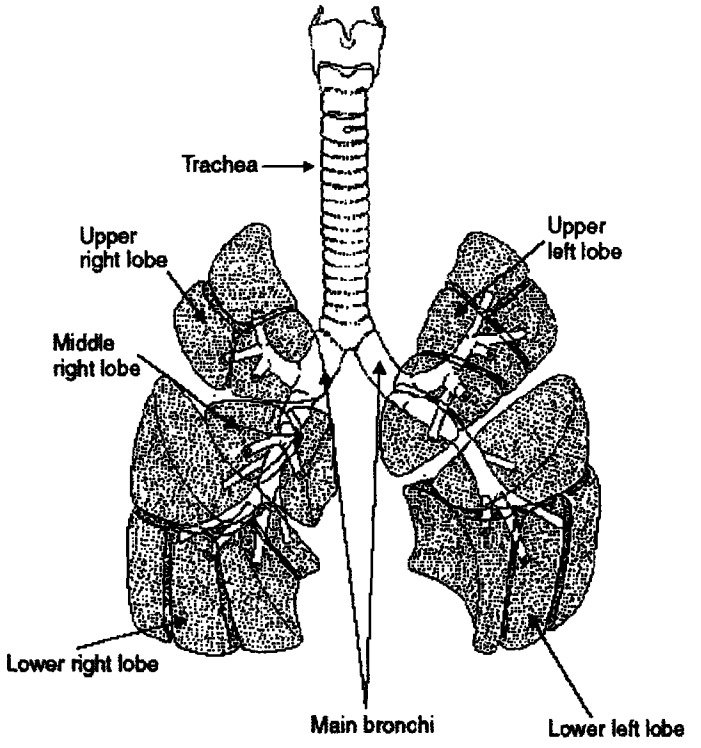

Figure 1 Gross anatomy of the lung [6]

The central airways are considered to be the trachea, right and left main bronchi, and the major lobar bronchi. The main distinguishing features of the airways are the presence of cartilage which forms a U-shaped structure anteriorly with the fibrous posterior membranous sheath. Between the central and distributing airways are numerous segmental bronchi and subsegmental bronchi. The distributing airways have a central diameter of 3-4 mm with regular U-shaped cartilage distinguishing them from the peripheral airways which have abundant smooth muscle in place of irregularly spaced cartilage. The terminal bronchioles are distinguished from the upper respiratory system

by their lack of cartilage. Following the terminal bronchioles are the respiratory bronchioles which contain scattered alveoli. The respiratory bronchioles further divide into alveolar ducts and alveoli. This branching tree structure of the lung allows the cross-sectional area to increase from the size of a quarter at the trachea to the size of half a tennis court at the alveoli (**Figure 2**). Gas exchange of carbon dioxide and oxygen from blood to the alveolar air occurs via molecular diffusion at the alveoli. For sufficient gas exchange, there are over 20 million alveoli in an adult human lung.

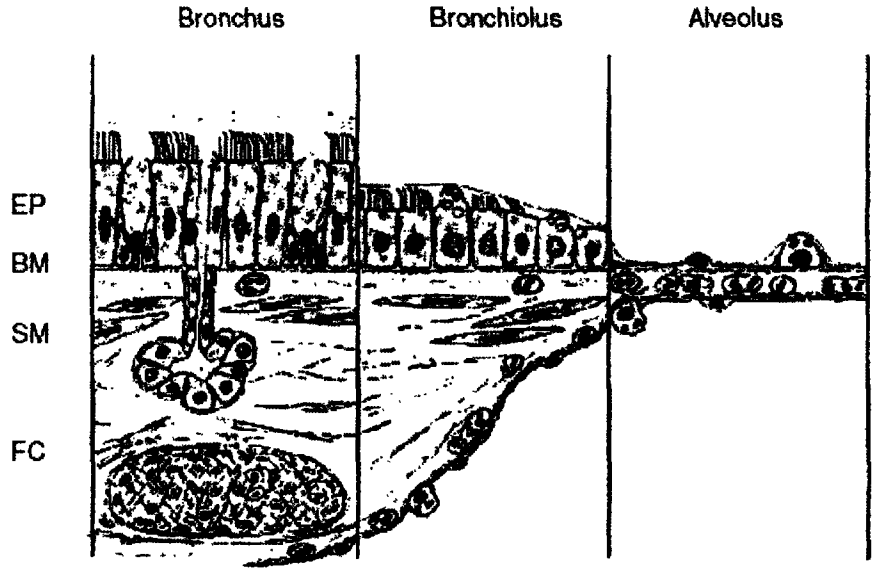

Figure 2 Schematic diagram of the branching structure of the lung (EP: epithelial layer; BM: basement membrane; SM: smooth layer; FC: fibrous coat). [6]

1.2.3 Structure-function relations

The alveolar tissues are mostly composed of elastin and collagen. Elastin is a cross-linked, random-coil protein that gives lungs their elasticity. The elastic fibers are arranged in a geodesic network that stretch and store energy during inspiration so that the lungs can passively deflate and recoil during expiration when the inspiratory muscles relax. Collagen is a crystallite that gives lungs high tensile strength. The collagen fibers form a second geodesic network around the alveolar epithelium as tissue stabilizing forces and prevent the lungs from overinflating.

The alveoli are the main gas exchange units and function to bring oxygen from the atmosphere to the blood and carbon dioxide from the blood to the atmosphere. Gas exchange through molecular diffusion is a slow process, and to ensure that there is

sufficient gas exchange to meet the body's demands, there needs to be maximal surface area for contact with the blood, minimal diffusion distance between the blood and air, and well mixing of gases in the lung. The alveoli are structured such that all these requirements are met. First, each alveolar wall is next to a blood vessel so that the diffusion distance between the alveolar epithelium to the endothelium is less than 5μm. Second, a large number of blood vessels line each alveolar space to maximize blood-gas contact. Third, the size of the each alveolus is only 200μm in size allowing well-mixing of the gases in the small space.

1.2.4 Histology of the lung

It will be important to identify the critically distinguishing histological features of the alveoli in order to determine the success in engineering this portion of the lung tissue. Typically, in vivo, the septae between adjacent alveoli contain a dense network of capillaries supported by collagen and elastin fibers. This layer of vessels and connective tissue is covered on either side by an exceedingly thin pulmonary epithelium made up of type I and type II alveolar cells. In thin portions of the alveoli, the basement membrane of the endothelium is fused with the basement membrane of the epithelial cells. In thicker regions, a pulmonary interstitium separates the interstitial space between the endothelium and the epithelium and contain elastin, collagen, fibroblast-like interstitial cells, smooth muscle cells, mast cells, and a few lymphocytes and monocytes. The epithelium is comprised of two types of cells – squamous, attenuated type I alveolar cells (pneumonocytes) and cuboidal type II alveolar cells. Type I cells function as the site of gas exchange between the blood and alveolar air and as the site for fluid absorption from the alveolar space. The role of the type II alveolar cell is in the production of surface-active phospholipids associated with the pulmonary surfactant system (discussed in **Appendices A.1**). Type I and type II alveolar cells make up 10% and 12% of the lung cell population respectively. Although the number of type I and type II cells are roughly equal in the alveoli, type I alveolar cells measure approximately 50μm in diameter and hence cover 95% of the alveolar surface while type II alveolar cells measure approximately 9μm in diameter and cover less than 5% of the alveolar surface. Alveolar

macrophages are also loosely attached to the epithelium and lie freely within the alveolar spaces.

Alveolar epithelial type II cells have microvilli on their apical surface, osmiophilic lamellar bodies in their cytoplasm, and form intercellular junctional complexes. Microvilli are covered by a blanket of glycocalyx that consists of delicate branching filaments of the terminal oligosaccharides of integral membrane proteins that project from the tip of the microvilli into the lumen. By providing a "diffusion barrier" the glycocalyx is thought to play a passive role in development of the epithelial barrier and host defense. However, neither the exact chemical composition nor the exact function of the glycocalyx is currently known. The osmiophilic lamellar bodies (OLBs) are a characteristic structural feature of type II cells and are dense granular regions with a limiting membrane. Its substructure consists of electron-opaque lamellae 26 angstroms thick with 16 angstroms wide electron translucent zones [7]. These cytoplasmic bodies are the source of surfactant production in the lung. Type II cells also contribute to epithelial repair through proliferation, differentiation into type I cells, and elimination of apoptotic alveolar epithelial type II cells by phagocytosis. Type II cells may also act as immunoregulatory cells.

Cell-matrix interactions play an important role in cellular function, secretion, and differentiation. The extracellular matrix (ECM) provides cells with structural support and modulates cell proliferation, cell migration, attachment, differentiation, and repair. The ECM of the lung is comprised of collagens, elastin, proteoglycans, glycoproteins, and basement membranes. Basement membranes are made of type IV collagen and laminin and separate the epithelium from the stroma. The function of basement membranes is to provide physical support to the cells resting on them and as a site for cell attachment. Most importantly, basement membranes are synthesized by the epithelial cells resting on them. Type I epithelium predominantly overlies a basement membrane comprised of type IV collagen, laminin, fibronectin, entactin, tenascin, heparan sulfate, and chondroitin sulfate proteoglycans [8]; whereas type II cells are interspersed in alveolar corners and lie above type I collagen as well as the other matrix components. In this study, the type I collagen-GAG matrix is used as a natural analog to the ECM.

1.3 Hypothesis, Objective, and Specific Aims

From work done by other investigators, type II alveolar cells can reaggregate to form alveolar-like structures suggesting the possibility for lung tissue engineering [9, 10]. The hypothesis is that lung tissue structures can be regenerated *in vitro* by fetal or neonatal rat lung cells grown in a collagen-GAG scaffold. Regeneration of lung tissue is expected to be histologically similar to lung tissue found *in vivo*. Lung tissue developed *in vitro* should have both alveolar type I and II cells, and cells should secrete extracellular matrix components found in the lungs. Both type I and II cells should also be morphologically similar to typical alveolar pneumonocytes. Type I cells are expected to be squamous, thin, with an attenuated nuclei, and type II cells are expected to be cuboidal, with characteristic osmiophilic bodies which secrete pulmonary surfactant.

The objective of this thesis project is to develop an *in vitro* system for the regeneration and long-term maintenance of lung tissue structures cultured in a collagen-GAG scaffold suitable for lung tissue engineering. The long-term goal is to develop a collagen-GAG scaffold as an implant to be used alone or seeded with cells for the regeneration of lung tissue *in vivo*.

Specific aims for this project include:

1. Development of a cell isolation procedure whereby cells are enzymatically dissociated from fetal and neonatal rat lungs while maintaining cell surface receptors which are critical in regeneration of lung structures.
2. Investigation of the effects of selected scaffold design variables on lung tissue regeneration in our *in vitro* system.
3. Investigation of lung cell behavior revealed as the cells interact with an analog of the extracellular matrix.
4. Identification of differences in fetal and neonatal lung cell behavior using histological analysis.

Chapter 2 Review of Past Work

2.1 Cell Source

Cells isolated from fetal rats appear to play an important role in the ability of type II alveolar cells to proliferate in tissue culture. In previous work, type II cells isolated from adult animals have exhibited minimal proliferation in tissue culture, and the addition of growth factors did not increase cell number. Confluent monolayers of adult type II cells formed by cell flattening and spreading rather than by cell division. Most *in vitro* studies reported only increases in DNA synthesis and changes in phenotype in the absence of proliferation. ECM preparation from bovine corneal endothelial cells and various soluble factors (rat serum, epidermal growth factor, insulin, cholera toxin) stimulated [^{3}H]thymidine incorporation, cell labeling, and DNA content. However, these agents did not affect cell proliferation since no increase was found in cell number. Unlike type II cells isolated from adult animals, fetal lung cells obtained from cultures of dissociated alveolar-like structures have been reported to have the capacity to proliferate.

2.2 Isolation Methods

There have been several *in vitro* techniques for the dissociation of lung tissue into a cell suspension used by various investigators. In particular, most investigators have focused on techniques to yield a purified population of alveolar type II epithelial cells for the purpose of studying pulmonary surfactant secretion.

One method of isolating type II epithelial cells is by differential adherence. Differential adherence in monolayer culture is used to separate epithelial cells from other cells found in the lungs. Fibroblasts typically adhere first to tissue culture surfaces, followed by macrophages and endothelial cells, and then type II cells. In the presence of serum, type II cells adhere more rapidly than most lymphocytes. The time period for type II cell adherence ranges between 3-48 hours. Therefore, a cell suspension of type II cells in high yield can be obtained by first plating the primary cell suspension on a tissue culture plate for one hour to remove most fibroblast cells, and then replating the non-adherent cell suspension and medium onto a new dish and culturing for one hour to

remove the endothelial cells and macrophages. After this second culture period, the medium and non-adherent cells can be resuspended and cultured for 1-2 days to allow the epithelial cells to adhere. In this manner, type II cells in greater than 90% purity can be obtained from 19-day fetal lungs [11, 12].

Another method for isolating type II epithelial cells is by using elastase, Immunoglobulin G, and "panning." Enzymatic digestion of lung tissue with trypsin or collagenase liberates alveolar cells as well as both interstitial and endothelial cells. Elastase is therefore used by other investigators to selectively loosen or remove the alveolar epithelium from the underlying basal lamina. It has also been documented that cell yield can be improved when elastase is used in addition to trypsin (50μg/ml crystalline trypsin is added to elastase 30 orecein/elastin U). The use of elastase instead of or in addition to trypsin is believed to better preserve an intact cellular membrane function [6]. IgG is plated onto the flasks for further selective removal of macrophages, leukocytes, fibroblasts, and non-type II cells [10, 13]. Since epithelial cells lack the Fc receptor which binds IgG, the adherent fibroblasts, macrophages and lymphocytes can be selectively removed.

2.3 ECM analogs used

Alveolar-like structures have been observed in previous work done using Gelfoam sponges [14], endothelial matrices [15], Matrigel, and floating collagen gel membranes [16]. Gelfoam sponges are made of gelatin and Matrigel is an epithelial basement membrane material rich in collagen IV and laminin. No information was given about the specific type of collagen in the Gelfoam sponges or floating collagen gel membranes used. In addition, other matrices previously used include rat tail collagen gels [16], human amniotic membrane [17], fibroblast feeder layers on collagen gels, preparations of alveolar basement membrane [17], and gels made of Engelbreth-Holm-Swarm (EHS) tumors [18].

2.4 Formation of Alveolar-Like Structures

Formation of alveolar-like structures composed of type II alveolar cell aggregates have been found by several investigators. One of the earliest documentation describing

the formation of these structures was by William Douglas in 1976 [9, 19, 20]. Douglas et al. observed the formation of histotypic structures from monodispersed fetal rat lung cells cultured in a three-dimensional Gelfoam sponge. He used lung cells obtained from 19-21 days gestation Sprague-Dawley fetal rats. The alveolar-like structures formed were noted to be composed of type II cell aggregates surrounding a central lumen [14]. The type II cells were cuboidal with lamellar bodies and intercellular tight junctions, and exhibited polarity with apical microvilli facing the lumen, basally located nuclei, gel matrix abutting the basal surface, and the cells secreted pulmonary surfactant confirmed by presence of osmiophilic lamellar bodies [7].

Sugihara et al. more recently also observed the reconstruction of alveolar-like structures from alveolar type II epithelial cells when cultured in a three-dimensional collagen gel matrix [10]. Lung cells were obtained from 21- to 23-days-old Wistar rats. A different method of isolation was used where elastase was used in tissue digestion. Cells were seeded by mixing the isolated suspension with a soluble type I collagen solution and warmed to form a gel. Sugihara et al. found that isolated type II cells reconstructed to form large alveolus-like structures composed of cells described morphologically as type I and type II cells.

In another study, investigators were able to obtain alveolar-like structures within 20 hours of cultures. Fetal rats between 18 to 22 days gestation were used. Lungs were dissected from the fetuses, minced, and then dispersed into a cell suspension using 0.05% trypsin and 10μg/ml DNase. Single cells were obtained by filtering the cell suspension through a 50μm Nitex filter. The cells were pelleted by centrifugation, incubated for 1 hr. at 37°C to allow reaggregation, and then resuspended in minimal essential medium (MEM) containing 10% fetal calf serum, 50μg/ml gentamycin, and 2.5μg/ml amphotericin B. An aliquot (75μl) containing approximately 10^7cells was inoculated onto 1cm^2 piece of medium hydrated Gelfoam and incubated overnight in 100mm Petri dished (10 – 15 pads per dish) containing 10ml of culture medium at 37°C in 5% CO_2 in air. Under these conditions, type II cells reaggregated as alveolar-like structures. [21]

Chapter 3 Materials and Methods

3.1 Fabrication of Type I Collagen-GAG Scaffold

The general paradigm of tissue engineering is to use a cell source, biomaterial scaffold, and bioreactor. Typically, cells (from living tissue or endogenous cells of the host) are seeded within a two-dimensional or three-dimensional biomaterial and cultured within a bioreactor to regenerate tissue *in vitro* which is then implanted *in vivo* as a reparative therapy to replace lost tissue and function. The biomaterial used is a scaffold that can be composed of natural polymers or synthetic polymers. Natural materials include proteins, such as collagen, fibrin, silk, and polysaccharides such as glycosaminoglycan and dextran. Synthetic polymers include poly(α-hydroxyesters) such as poly(glycolic acid), poly(L-lactic acid), poly(lactic-co-glycolic acid), or hyaluronan derivatives. The scaffold plays a key role in tissue engineering and provides a three-dimensional environment for the cells. Ideally, the scaffold represents an analog of the *in vivo* extracellular matrix structurally and chemically at the molecular, micro-, and macro-level.

Collagen is a triple helical protein abundant in the connective tissues of the body (**Figure 3**). Its primary structure is a polypeptide chain $(Gly\text{-}X\text{-}Y)_n$ rich in proline and hydroxyproline with glycine at every third amino acid allowing the polypeptide to undergo rotation. The secondary structure is helical due to the hinge-like glycine and stiff hydroxyproline units. Three secondary helical polypeptides form the tertiary triple-helical collagen molecule which is 1.5nm in diameter and 300nm in length and bundle into microfibrils 4nm in diameter. These microfibers then bundle into fibers 0.5μm in diameter. The quaternary structure of collagen is highly specific forming a crystalline fiber with a banding pattern of 64-nm periodicity (**Figure 4**). Collagen's functions originate from its unique primary to quaternary structure and its architecture. Advantages of collagen scaffolds are their very mild inflammatory response across species, high porosity, controllable pore size, and degradation by tissue collagenases. Limitations to collagen scaffolds include mechanical instability compared to stronger scaffolds (silk, polymers), contraction over time due to dehydration of collagen fibrils, structural heterogeneity, and possible pathogen transfer.

Figure 3 Triple helical structure of collagen

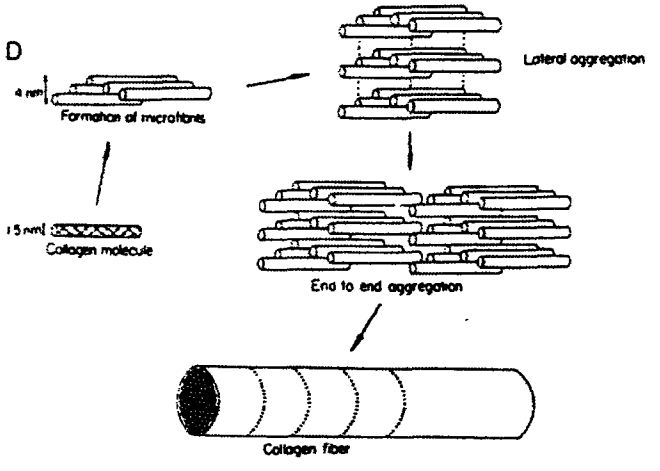

Figure 4 Tertiary protein structure of collagen molecule which aggregate to form microfibrils. Microfibrils bundle laterally and end to end into the quaternary structure of collagen fibers with 64-nm periodicity.

Highly porous scaffolds are used in tissue engineering to provide both a three-dimensional environment for cells and a high surface area to allow cell attachment and cell-scaffold interactions. The porosity and pore size of the scaffold determine the area available for cell attachment, migration, and mass transfer. It has been shown that cell-scaffold interactions play an important role in cellular activity and processes. Optimally, in order for the scaffold to promote cell adhesion and cell growth, the chemical composition of the scaffold should contain ligands that allow cell adhesion and have pore sizes large enough for cells to migrate in. The scaffold should also be highly porous so that nutrients and metabolites can diffuse freely through. Typically cells are 90-99% porous with pore diameters that range 5-500μm.

The scaffold also needs to satisfy conditions for *in vivo* implantation. The scaffold must not only promote cell activity *in vivo*, but must also be biocompatible in the

body and biodegrade to minimize long-term immunogenicity. The degradation rate of the scaffold *in vivo* should match the rate of tissue regeneration so that the scaffold only serves as a cell delivery device or provides mechanical structure during the duration of critical cellular processes and then degrades into biocompatible products. The scaffold degradation time is dependent on many variables including degree of cross-linking, mechanical factors, molecular and structural characteristics of the scaffold, cell-seeding density, and the extracellular environment.

The scaffold fabricated in this study allows the transport of cells and metabolites through a large pore volume fraction and an interconnected pore network. High cell attachment is achieved through a high specific surface area (high surface area to volume ratio), which is dependent on scaffold pore size, pore shape, and pore volume fraction. Ideally, the optimal fabrication should produce a scaffold that is homogenous in pore size and shape.

3.1.1 Fabrication of scaffold

Type I collagen-glycosaminoglycan scaffold was fabricated from type I slurry using a freeze-drying method [22]. The suspension was made from dry type I collagen isolated from bovine tendon (Integra Life Sciences, Plainsboro, NJ), chondroitin-6-sulfate isolated from shark cartilage (Sigma Aldrich Chemical Co., St. Louis, MO), and 0.05M acetic acid (pH 3.2). The final suspension contained 0.5wt% type I collagen, and 0.05wt% chondroitin-6-sulfate. The slurry was first cooled to 4°C to prevent denaturation of collagen fibrils, and then mixed with a blender at 15,000rpm. The final suspension was degassed at a pressure ~50mTorr for 90 minutes to remove air bubbles created with the blender before freeze-drying.

A volume of 67.25ml of degassed collagen-glycosaminoglycan (GAG) suspension was used to fabricate one sheet of scaffold 12.4 x 12.4cm. The suspension was first equilibrated to 20°C within the freeze dryer oven for 5 minutes. The temperature of the freeze dryer chamber was then reduced and ramped down to -40°C to produce solidified collagen-GAG co-precipitate localized between nucleated ice crystals. This network of ice and co-precipitate was then annealed at that temperature for a minimum period of 60 minutes to allow the ice crystals that nucleated to grow. After this

annealing period, the ice crystals were sublimated under vacuum (<100mTorr) at 0°C for 17 hours to leave behind a highly porous solid type I collagen-GAG scaffold.

3.1.2 Pore Size and Porosity

The fabrication protocol described above creates a collagen-GAG scaffold with uniform porosity of 99.5%. The pore size of the scaffolds can be altered by changing the annealing temperature and ramping time. Larger average pore sizes can be created by increasing the annealing temperature, decreasing the ramping time, and decreasing the total time from start to sublimation. In this manner, larger ice crystals can be formed and sublimated producing a scaffold with a larger average pore size. In the studies done, scaffolds with an average pore size of 95.9±12.3μm, 99.5% porosity, and a specific surface area (S.A./Vol) of 0.00748μm^{-1} were used as well as scaffolds with an average pore size of 109.5±18.3μm, 99.5% porosity, and a specific surface area of 0.00655μm^{-1}. The table below provided by Brendan Harley [22] reflects the effect of time and temperature on pore size.

Table 1 Scaffold Pore Size vs. Ramping Time and Temperature

Average Pore Size (μm)	Ramping & Annealing Temperature (° C)	Ramping Time (min)
95.9±12.3	-40	15
109.5±18.3	-30	10
121.0±22.5	-20	10
150.5±32.1	-10	5

3.1.3 DHT cross-linking

The collagen-GAG scaffolds were dehydrothermally (DHT) cross-linked to increase the mechanical properties of the structure. Scaffolds were cross-linked under vacuum at 50mTorr at 105°C for 24 hours in a vacuum oven (Fisher IsoTemp 201, Fisher Scientific, Boston, MA). DHT-treatment of scaffolds covalently cross-links the polypeptide chains of the collagen fibers without denaturing the collagen into gelatin. Treatment of the scaffolds at high temperature also renders the scaffold sterile without changing its physical and chemical structure.

3.1.4 EDAC cross-linking

To decrease the degradation rate of the collagen-GAG scaffolds, scaffolds were chemically cross-linked by 1-ethyl-3-(3-dimethylaminopropyl)carbodiimide (EDAC) cross-linking. DHT-treated matrices were first hydrated with half the total final volume of EDAC (MW = 191.7g/mol; Sigma Aldrich Chemical Co., St. Louis, MO) and N-hydroxysuccinimide (NHS) (MW = 116g/mol, Sigma Aldrich Chemical Co., St. Louis, MO). 6mmol EDAC/g collagen was used with a 5:2 molar ratio of EDAC: NHS dissolved in distilled water. Matrices were chemically cross-linked at room temperature for 15 to 20 minutes, washed with Hank's Balanced Salt Solution, and rocked on a nutator for at least an hour to remove residual NHS/EDAC solution. Matrices were rinsed in sterile deionized water before use.

3.1.5 Experimental preparation

Type I collagen-GAG sheets (12.4cm x 12.4cm x 2cm) were punched from the dry sheets of the scaffold samples, 8mm in diameter x 2 mm in thickness, using a sterile dermal punch (Barron Vacuum Trephine, 8mm, Katena Products). Prior to cell-seeding, matrices were hydrated in sterile deionized water and rocked on a nutator to remove any bubbles for at least an hour at room temperature. Matrices were then hydrated in warmed (37°C) media before direct cell-seeding.

3.2 Isolation of Rat Alveolar Cells

3.2.1 Cell Source

For this thesis, lung cells were obtained from the following animals with the approval of the VA Animal Care Committee: 10-day-old mice, 16 to 20-days gestation fetal rats, and 2-day-old neonatal rats. The 10-day-old mice were provided by Boston University. Neonatal and fetal lung cells were obtained from timed-pregnant Sprague Dawley outbred rats (Taconic, Germantown, NY). It is still not possible to determine with complete accuracy the time of conception. However, the time of egg and sperm fertilization can be determined within a 24-hour window of accuracy by detection of sperm in the female. By convention, fertilization marks the beginning of day 1 of

gestation. Fetal rats 19 days of gestation mark 18 days after the day of conception. Typically, the term averages 22 days but can range between 21-23 days. The developmental stages of fetal rats have been well documented. By day 19, the embryo has undergone nearly complete maturation, eye lids are formed and fused (day 15), joint cavities have developed for the shoulder, elbow, hip, and knee joints (day 16), for the carpal and tarsal joints (day 17), and for the digital joints of the legs (day 19). At 19 days of gestation, all blood activity still occurs in the liver. By day 22, blood forming activity in the liver ceases with the end of gestation. At birth the crown to rump length of the fetus ranges from 40.5mm to 42.6mm and weight 5.9 – 6.4g.[23]

3.2.2 Methods for Cell Isolation Procedure

The isolation of rat alveolar cells from the lung tissue is a critical process to the reaggregation and regeneration of cells into alveolar-like structures. Successful structural formation and lung tissue regeneration is not only dependent on its environment but also on the retention of cell surface receptors that enable cell recognition and migration. Improper tissue dissociation methods can damage cell surfaces, destroy these receptors, and ultimately reduce cell viability. Hence, the method used in this study is documented in detail.

3.2.2.1 Dissection

Lungs cells were isolated using a modified method from work done by Douglas et al [24]. A timed-pregnant female rat (Taconic) was first sacrificed by CO_2 asphyxiation between 19-20-days gestation. A hysterectomy was then performed and the fetuses were aseptically removed from the uterus and washed with Hank's Balance Salt Solution (HBSS) (Gibco). The fetuses were dissected free of the placenta and attendant membranes, and the umbilical cords were cut. After washing with fresh HBSS, the thoracic cavity was exposed and the lungs were perfused with 3ml of HBSS via a 27-gauge needle placed in the right ventricle until the blood cleared and was then excised. Lungs were then removed from each fetus and washed in serum-free Kaighn's modified F12K medium.

3.2.2.2 Tissue Homogenization and Digestion

Lung tissues were first minced into 1mm^3 pieces using a sterile razor blade under sterile conditions. Tissue was then digested using 30ml of sterile CTC enzyme solution containing 0.1% type I collagenase [155units/mg] (Gibco), 0.1% trypsin buffer (Sigma), 1% chicken serum in 1X calcium and magnesium-free Dulbecco's phosphate-buffered saline (Gibco) and 500µl RNase-free DNase [1000units/ml] (Promega) with 29.5ml of HBSS (Gibco). DNase was used to prevent the polymerization of DNA released from damaged cells. This solution was placed on a shaker and incubated for 15 minutes at 300rpm, 37°C. The dissociation fluid was filtered through a 41µm-pore size mesh. The remaining tissue was washed with serum-free F12K media filtered through the mesh. Lung tissue and solution were stored on ice to lower cellular metabolism and prevent cell autolysis. Fetal bovine serum (FBS) was added to inactivate the collagenase and trypsin. An additional 30ml of CTC enzyme solution and 1000units DNase was then added to the undigested tissue and the solution was incubated on a shaker for another 15 minutes at 300 rpm, 37°C. The digested solution was also filtered through the 41µm-pore size mesh (Spectra mesh, VWR). F12K supplemented with 10% fetal bovine serum (FBS) was then added to inactivate the trypsin and collagenase for a final volume of 50ml. The harvested cell suspension was centrifuged for 10 minutes at 1500rpm and the supernatant removed leaving several milliliters of supernatant medium. Cells were resuspended by mild Vortex mixing and the solution was then passed through a 25µm filter (Spectra mesh, VWR). This homogenate was centrifuged for 10 minutes at 1500rpm and the supernatant discarded leaving a thin layer of medium above the pellet. The cell pellet was incubated at 37°C for 1 hour. (Refer to Protocol **A.2** in **Appendix** section for more details.)

Lung cells were isolated from mice and neonatal rats by a method similar to that described above. However, mice and rats were first anesthetized intraperitoneally with 0.15ml of sodium pentobarbital.

3.3 Cell seeding and Culture

Prior to cell seeding, a viable cell count was first performed using trypan blue exclusion. Cells were seeded using the pipette method. The F12K or Ham's media (Gibco) used was supplemented with 10% fetal bovine serum (Gibco), 1% antimyotic

(Gibco), and 2% penicillin-streptomycin-glutamine (Gibco). Following the one hour incubation period, cells were resuspended in medium to give a final concentration of 10^8cells/ml. Cells were seeded with a cell-seeding density of $5x10^6$cells/matrix or with a minimum of $1x10^6$cells/ matrix in agarose-coated 12-well tissue culture plates. Each side of the matrix was inoculated with 20µl of cell suspension or complete media for the controls. Matrices were incubated for 10 minutes and the other side was then inoculated with an equal amount of cell suspension or complete media. Matrices were then incubated for 2-3 hours to allow cells to attach to the substrate before adding 0.5ml of complete media. After 24 hours, 1.5ml media was added to each well, and after 48 hours, cultures were placed on a rocker platform at a speed of 6 cycles per minute. Complete medium is replaced every 2-3 days.

3.4 Histology & Immunohistochemistry

3.4.1 Fixation

Matrices were removed from media and fixed in 10% neutral buffered formalin for a minimum period of 24 hours before processing. Fixation is needed to prevent autolysis and preserve cells and tissues permanently in as life-like state as possible. Formalin (formaldehyde) is an aldehyde which fixes tissues by reacting primarily with basic amino acids to form cross-linking methylene bridges without significantly altering the structures of intracytoplasmic proteins. Buffer is used to prevent acidity that would promote cell autolysis and precipitation of formol-heme pigment in tissues.

3.4.2 Processing, Embedding, Sectioning

Samples were processed to get fixed-tissue into paraffin. Processing was done using an automated tissue processor. During processing, matrices were dehydrated using ethanol and cleared using xylene. After processing, samples were embedded in paraffin and sectioned 7µm thick using a microtome.

3.4.3 Staining

To prepare matrices for staining, samples must first be deparaffinized to allow water soluble dyes to penetrate. Samples were deparaffinized in xylene and then

rehydrated in 100%, 95%, 80%, and 70% ethanol and stained. Samples were then dehydrated in 80%, 95%, and 100% ethanol, xylene, and coverslipped (mounting media Cytoseal 60).

3.4.3.1 Hematoxylin & Eosin

To observe the presence of cells in the matrices, hematoxylin & eosin stain was used. Hematoxylin is a basic dye that stains blue-purple and eosin in an acidic dye that stains pink-red. Eosin stains proteins and cytoplasm while hematoxylin stains anything negatively charged including the nucleus and DNA. Differentiation between type I and II alveolar cells can also be determined through hematoxylin and eosin staining. Type II alveolar cells should appear cuboidal in shape with microvilli on their apical surface while type I alveolar cells should appear attenuated and squamous and lack microvilli.

3.4.3.2 Smooth muscle actin

Smooth muscle actin is a protein filament important to cell contraction and migration. Myosin-actin interactions are responsible for generating tensile and contractile forces within the cell. Immunohistochemistry is performed to detect presence of α-smooth muscle actin in cell-seeded scaffolds.

Samples were first deparaffinized in xylene and rinsed in absolute alcohol followed by distilled water. Sections were then incubated in TRIS/HCl buffered saline, pH 7.6 (TBS) followed by 3% hydrogen peroxide (H_2O_2) solution to quench endogenous peroxidase activity and reduce background staining. Slides were washed with TBS before adding protein blocking agent (PBA) to reduce non-specific antibody binding. Sections were incubated in primary α-smooth muscle actin antibody for 1 hour. After washing in TBS, biotinylated secondary antibody was added. After one wash with TBS, peroxidase reagent was added followed by a second wash with TBS. Sections were then incubated in DAB developer solution, washed in TBS and counterstained in hematoxylin.

3.4.3.3 Cytokeratin

Cytokeratin is an intermediate filament specific to epithelial cells and can be used to differentiate epithelial cells from cells of other origins. Immunostaining for monoclonal antibody to cytokeratin is used to identify epithelial cells. Cells are stained

for cytokeratin using anti-cytokeratin solution diluted 1:5 in using a similar method described in **3.4.3.2**. Type II cells are known to be positive for monoclonal antibody to cytokeratin no. 19 and type I for cytokeratin no. 18 [21].

3.4.3.4 Elastin

Elastin is abundant in the extracellular matrix of the lung *in vivo*. Dye to identify the presence of elastin is made using 1g hematoxylin powder, 100ml of 100% ethanol and ferric chloride. The dye is differentiated using saturated picric acid and van Gieson stain is used to provide contrast.

3.4.3.5 Masson Trichrome

Masson Trichrome is a connective tissue dye. It is a three dye stain that stains the cell nuclei black, the cell cytoplasm red, and collagen blue.

3.5 Experimental Design

To study the influence of the extracellular matrix on lung tissue engineering, both DHT-treated and EDAC-treated matrices were initially used. EDAC matrices prevent contraction, have a lower degradation rate, and provide a stronger substratum support for cells. DHT-treated matrices have a higher degradation rate and are more similar to the Gelfoam matrices or floating collagen membranes previously used in other work. Using two types of matrices allows exploration of the importance of contraction and the effect of degradation rate on the formation of alveolar-like structures.

3.5.1 Mice studies

Two studies were performed using lung cells obtained from newborn mice 10-days-old. In the first study, lung cells from 13 pups were obtained, and in the second study, lung cells were obtained from 11 pups. Cell isolation procedure is described in **Chapter 3**. Mice were provided by Boston University. Cells were seeded into both DHT-treated (105°C, 24hrs) and EDAC-treated type I collagen-GAG matrices. Type I collagen-GAG matrices had an average pore size of 95.9±12.3μm, porosity of 99.5%, and specific surface area of 0.00748μm^{-1}. Matrices were pre-hydrated before seeding by the pipette method. Following the study by Douglas[20], a cell-seeding density of

$5x10^6$cells/matrix was used. Due to a fewer number of cells obtained in the second study, a cell-seeding density of $2.6x10^6$cells/matrix was used. Samples were sacrificed and examined at 7 days, 14 days, and 21 days. The media used in cultures was DMEM/F-12 (Gibco) supplemented with 10% FBS and antibiotics.

3.5.2 Neonatal rat studies

Neonatal rats of Sprague Dawley strain (Taconic) were sacrificed when they were 2-days-old. Lung cells were obtained from a total of 13 rats. To increase the cell number, cells from 6 rats were plated and cultured for 1 week before seeding. Primary lung cells from 5 rats were directly seeded into collagen-GAG matrices. A total of 12 DHT-treated matrices were used with an equal number of experimental samples and controls. Type I collagen-GAG matrices had an average pore size of 95.9±12.3μm, porosity of 99.5%, and specific surface area of $0.00748\mu m^{-1}$. Matrices were pre-hydrated before seeding by the pipette method. The cell-seeding density determined prior to seeding was 3.07×10^6cells/matrix. Samples were sacrificed after 1 week, 2 weeks, and 3 weeks. The tissue culture was placed on a rocker platform and culture was rocked between 3-6 cycles/min to increase perfusion of nutrients and media through the matrix. Samples were analyzed by scaffold contraction, histology, and immunohistochemistry.

3.5.3 Fetal rat studies

Lung cells were isolated from fetal rats at 19 to 20-days gestation because this is during the saccular phase of lung development where respiratory endings expand to form saccules and differentiation between type I and II alveolar cells begin. However, due to continuing differentiation of cells at an unknown rate, the gestational age of the cells in the final culture cannot be related to that of the animals from which they were isolated.

3.5.3.1 16 days gestation

An initial study was performed using cells from fetal rats at 16-days gestation. Observations of lung cell behavior at 16-days gestation can be compared with cells obtained at a later gestational age to find the effect of gestation age on lung cell behavior. Lung cells were isolated from twelve fetal rats (Sprague Dawley, Taconic) at 16 days of gestation. Both DHT-treated matrices (n=4) and EDAC-treated matrices (n=4) were used

with a cell-seeding density of 2.3 x 10^6cells/matrix. Type I collagen-GAG matrices had an average pore size of 99.5±12.3μm, porosity of 99.5%, and specific surface area of 0.00748μm^{-1}. Matrices were pre-hydrated before seeding by the pipette method. Cultures were placed on a rocker after 48 hours at 6 cycles/ min. Samples were sacrificed after 1 week, 2 weeks, and 3 weeks. H&E and cytokeratin samples were examined using light microscopy.

3.5.3.2 19 days gestation

Lung cells were isolated from six timed-pregnant Sprague-Dawley rats and a total of 92 lungs were obtained. In this study, a total of 77 type I DHT-treated collagen-GAG scaffolds with pore size of 95.9±12.3μm. There was a total of 35 type I collagen-GAG cell-seeded matrices and 42 type I collagen-GAG controls. From data given by Douglas, we expected lung tissue from 100 19-20 days gestation fetuses to have a wet weight of 5g and a total of 175-200x10^7cells. Cells were isolated following the protocol described in **Chapter 3**. Matrices were seeded with a density of 3.98 x10^7cells/matrix. Samples were sacrificed at 2 days, 2 weeks, and 3 weeks and analyzed histologically (n=3). A DNA assay was also conducted to determine cell activity and proliferation (n=6).

Another study was conducted using the same variables described above with three timed-pregnant Sprague-Dawley rats and a total of forty-one 19-days gestation rats; however, matrices were seeded dry rather than hydrated. It was believed that while pre-hydrating the matrices had the advantage of removing bubbles within the matrix, if the matrix was saturated it would prevent cells from migrating in. In this study, the scaffold used were type I collagen-GAG with a pore size of 95.9±12.3μm. The tissue culture plates were placed on a rocker at 6 cycles/ min after 2 days for the remaining time in culture. From a cell-count performed, there were a total of 208.12x10^6 cells including the red blood cells. The cell-seeding density used was therefore 10.41x10^6cells/matrix. Cells were seeded into dry matrices using an aliquot of 40μl/matrix. The media used in this study was Ham's F12 media supplemented with antimycotic, penicillin, and 10% FBS. A total number of 38 scaffolds were used. Sample size for this study was n= 6 with an equal number of controls. Cells were analyzed by H&E, SMA, cytokeratin, and elastin histology stains.

3.5.3.3 20 days gestation

A study was conducted using fetal rats at 20-days-gestation. Lungs from a total of 35 fetuses were isolated. DHT-treated type I collagen-GAG matrices were used and samples were sacrificed at 3 days, 9 days, 2 weeks, and 3 weeks. Type I collagen-GAG matrices had an average pore size of 109.5±18.3μm, porosity of 99.5%, and specific surface area of $0.00655\mu m^{-1}$. Matrices were pre-hydrated before seeding by the pipette method. In this study, passaged cells and primary cells were used. In passaged cells, cells were cultured for 4 days before trypsinized and used for seeding. From a cell count performed, there were $17.52x10^6$ passaged cells with 74% viability and $8.96x10^6$ primary cells. A cell-seeding density of 1.12×10^6cells/matrix was used for seeding with primary cells and a cell-seeding density of 9.7×10^5cells/matrix was used for seeding with passaged cells. The difference in number reflects the number of red blood cells in the primary cell suspension that were directly seeded into the matrices as well. The entire study had a total of 34 cell-seeded matrices and 34 control matrices. Samples were sacrificed and analyzed for contraction, H&E, cytokeratin, SMA, and DNA.

3.6 DNA Assay

Samples were assayed for DNA to determine the cell count and cell proliferation activity. Samples were first lyophilized in the lyophilizer machine under vacuum below $133x10^{-3}$mbar overnight before digestion using 0.125mg papain (Sigma) per 6.25mg sample at 60°C overnight. Papain buffer solution was composed of 2.45ml dibasic stock solution, 17.54ml monobasic stock solution, 80ml distilled water, 87.82mg L-cysteine HCl, 186.12mg disodium ethylenediamenetetraacetate (EDTA, Fisher) adjusted to a pH of 6.2. Aliquots of papain digested samples were read fluorometrically using 1:200 pico-green dye dilution (Perkin Elmer Victor^2, $\lambda_{excitation}$= 485nm, $\lambda_{emission}$ = 535nm, 1.0s). The amount of DNA was then quantified by extrapolation from a standard curve of calf thymus DNA.

3.7 Collagen-GAG Assay

A collagen-GAG assay was performed to find any glycosaminoglycan content in the cultures. Samples were prepared in the manner similar to preparation for the DNA

assay. Aliquots of papain digested samples were read fluoremetrically using dimethylene blue. The amount of GAG was then quantified by extrapolation from a standard curve of shark chondroitin sulfate in dH_2O.

3.8 Quantification for Alveolar-like structures

The formation of alveolar-like structures was quantified using Scion Image (Scion Corporation; Frederick, MD). Since most of the alveolar-like structures were more elliptical than circular, two measurements were made in determining the size of the structures. The minor axis was defined as the smallest measured diameter and the major axis was defined as the largest diameter measured. Another term, the form factor, was defined as the ratio between the major and minor axis which can range between 0 and 1. A structure resembling a circle would have a form factor of 1 while the more elliptical the structure was, the closer the form factor would be to 0. The average size of the alveolar-like structures was taken to be the average between the major and minor axis, or the average between the largest and smallest diameters.

3.9 Pore Characterization

Scaffolds were embedded in paraffin, sectioned 7μm thick, and stained using hematoxylin and eosin. Samples were visualized on an optical microscope and digital images were taken using a color video camera. Images were first edited on Adobe Photoshop. Pore size of scaffolds was characterized from digital images using a linear intercept method macro from Scion Image image analysis software (Scion Corporation; Frederick, MD). The linear intercept method constructs a best-fit ellipse to analyze the average pore cross-section. The major and minor axes of the ellipse are multiplied by a factor of 1.5 to correct for pores that are not sectioned at the maximal cross-section but at an arbitrary angle. The average of the major and minor axes of the best-fit ellipse is defined as the mean intercept length. The mean pore diameter of the scaffold at each position within the scaffold is calculated from the average of the mean intercepts in the longitudinal plane and in the adjacent traverse plane [22].

3.10 Sample Size

The sample size for the analyses used was (i.e., n=6) based on the desire to determine as significant as 20% difference between experimental groups (control vs. cell-seeded) each with a 10% coefficient of variation when evaluating selected parameters (e.g., the number of alveolar-like structures formed per collagen-GAG sponge, scaffold contraction). A 15% standard deviation is assumed and alpha=0.05 and beta=0.1 is employed. Experiments were run in duplicate. Analysis of variance (ANOVA) was used to determine the effects of selected treatments on the outcome variables, followed by Fisher's least squares protected difference (LSPD) post-hoc test to compare specific groups.

Chapter 4 Results

4.1 Sample Size

A summary of the number of fetuses and neonates isolated from timed-pregnant Sprague-Dawley rats are shown in **Table 2**. Primary cells or both primary cells and secondary (passage 1) cells were used in the studies as indicated. The number of cell-seeded constructs sacrificed for histological analysis in each study is shown in **Table 3**. Cell-seeded samples were also for DNA analysis in studies using 19-days and 20-days gestation fetal rat.

Table 2 Number of timed-pregnant Sprague-Dawley rats and corresponding fetuses or neonates sacrificed for lung cells in each study.

	Timed-Pregnant Rats	Fetuses	Passage
16-days gestation	1	12	Primary
19-days gestation	9	133	Primary
20-days gestation	3	35	Primary and P1[1]
2-days neonatal	1	13 neonates	Primary and P1

Table 3 Number of cell-seeded type I collagen-GAG scaffolds sacrificed for histological and DNA analysis in each study.

	DHT cross-linked				EDAC cross-linked			
	2 days	1 wk	2 wks	3 wks	2 days	1 wk	2 wks	3 wks
Fetal								
16-days	–	4	4	4	–	4	4	4
19-days	16(6)[2]	–	15(5)	16(4)	–	–	–	–
20-days	7(3)	9(5)	10(5)	9(4)	–	–	–	–
Neonatal								
2-days	–	4	4	4	–	–	–	–

4.2 Controls

The controls used in the study were unseeded DHT cross-linked and EDAC cross-linked type I collagen-GAG matrices. Matrices were fabricated, cross-linked, and pre-hydrated as described in **Chapter 3**. Unseeded matrices were then incubated and

[1] P1 refers to passage 1 or the secondary cell culture derived from the primary cell culture after one subculture.
[2] Number of cell-seeded constructs allocated for DNA analysis appears in parentheses.

cultured in agarose-coated tissue culture plates with complete media at 37°C, 5% CO_2. Media was changed every 2 days. At the end of each time point, control matrices were fixed and stained for histological study. The pore structure and degradation of the matrices can be seen in **Figures 5-10.** Average pore size of matrices is tabulated in **Table 4**. Over time, matrices degraded by hydrolysis. Macroscopically, matrix diameter decreased over time. However, matrix pore size decreased from 1 week to 2 weeks in culture due to scaffold shrinkage and then pore size increased after 3 weeks in culture due to degradation of the collagen-GAG matrix (**Table 4**). Differences between DHT cross-linked matrices and EDAC cross-linked matrices are less significant than differences between prehydrated and dry DHT cross-linked matrices. Average pore sizes of dry DHT cross-linked matrices are larger than prehydrated DHT cross-linked matrices at 1, 2, and 3 weeks. However, the difference in average pore size is not significantly different at the 95% confidence level using a Fisher's LSPD analysis.

After 1 week in culture, pore sizes of DHT cross-linked (**Figure 5**) and EDAC cross-linked (**Figure 6**) matrices remain uniform. After 2 weeks in culture, pore sizes of EDAC cross-linked (**Figure 8**) matrices enlarge while DHT cross-linked (**Figure 7**) matrices diminish. This correlates with the decrease in scaffold diameter over time. By 3 weeks in culture, differences are even more significant (**Figure 9, 10**). EDAC treatment following DHT treatment maintains pore structure and architecture. A separate study was conducted to observe differences between DHT cross-linked matrices that were not prehydrated before incubating and culturing (**Figures 11-13**). The scaffold characteristics of these matrices differ from prehydrated DHT cross-linked matrices and appear similar to EDAC cross-linked matrices. Average pore sizes of dry DHT cross-linked matrices are larger than both prehydrated DHT and EDAC cross-linked matrices.

Pore sizes of matrices were characterized and results are tabulated below.

Table 2 Average pore diameter calculated using linear intercept method for DHT cross-linked and EDAC cross-linked matrices at 1, 2, and 3 weeks. N=1. [25]

Matrices Type	Time	Average Pore Diameter
Prehydrated DHT cross-linked	1 week	111μm
	2 weeks	102μm
	3 weeks	108μm
Prehydrated EDAC cross-linked	1 week	112μm
	2 weeks	102μm
	3 weeks	105μm
Dry DHT cross-linked	1 week	120μm
	2 weeks	115μm
	3 weeks	155μm

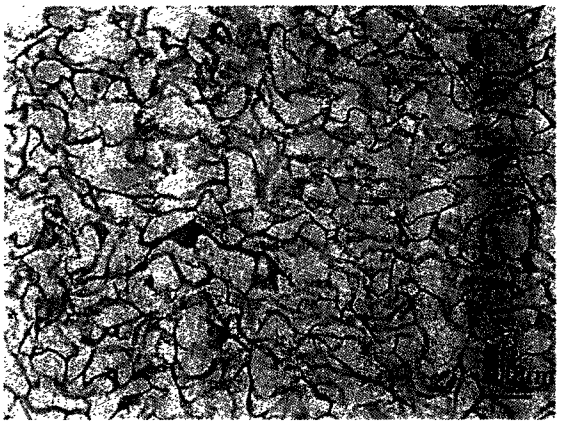

Figure 5 DHT-treated type I collagen-GAG scaffold after 1 week in culture. H&E; 100X.

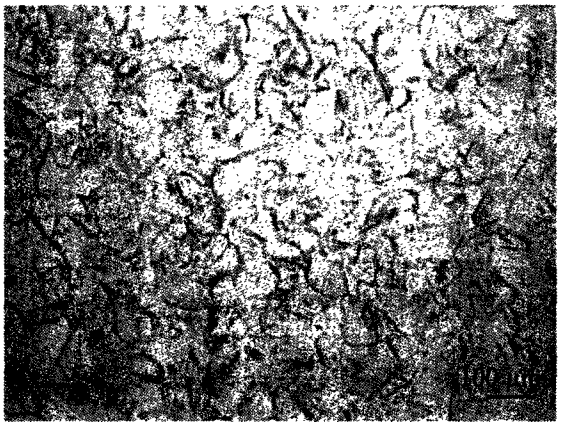

Figure 6 EDAC-treated type I collagen-GAG scaffold after 1 week in culture. H&E; 100X.

Figure 7 DHT-treated type I collagen-GAG scaffold after 2 weeks in culture. H&E; 100X.

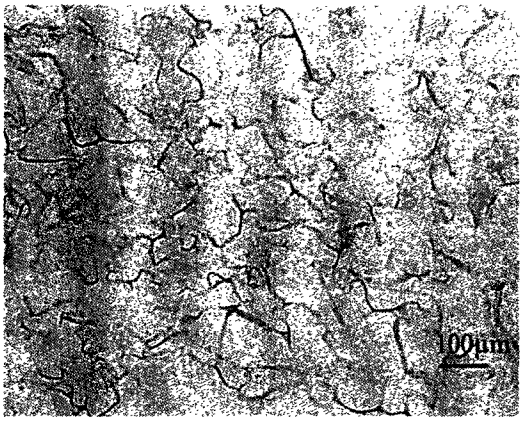

Figure 8 EDAC-treated type I collagen-GAG scaffold after 2 weeks in cultures. H&E; 100X.

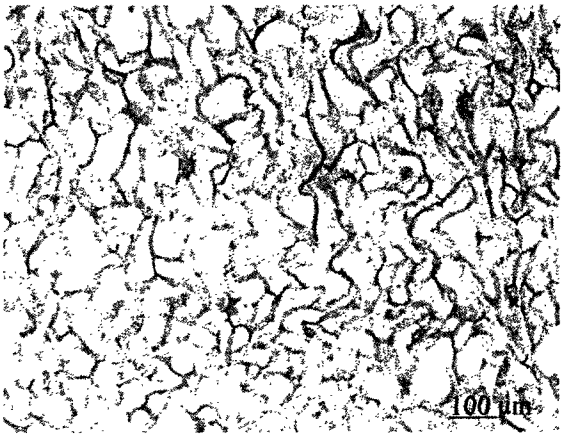

Figure 9 DHT-treated type I collagen-GAG matrix after 3 weeks in culture. H&E; 100X

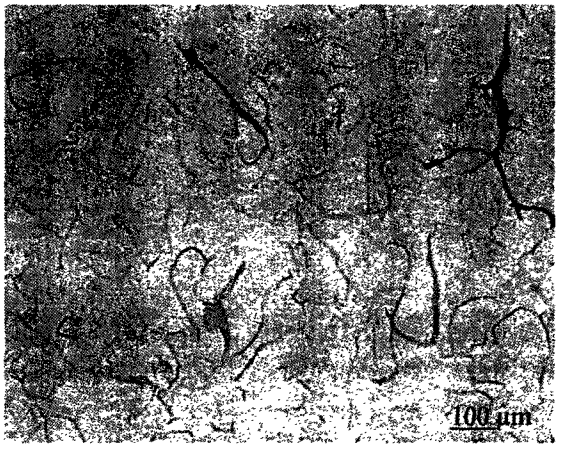

Figure 10 EDAC-treated type I collagen-GAG matrix after 3 weeks in culture. H&E; 100X.

Figure 11 DHT-treated type I collagen-GAG scaffold after 2 days in culture. Scaffold was not prehydrated. H&E; 100X.

Figure 12 DHT-treated type I collagen-GAG scaffold after 2 weeks in culture. Scaffold was not prehydrated. H&E; 100X.

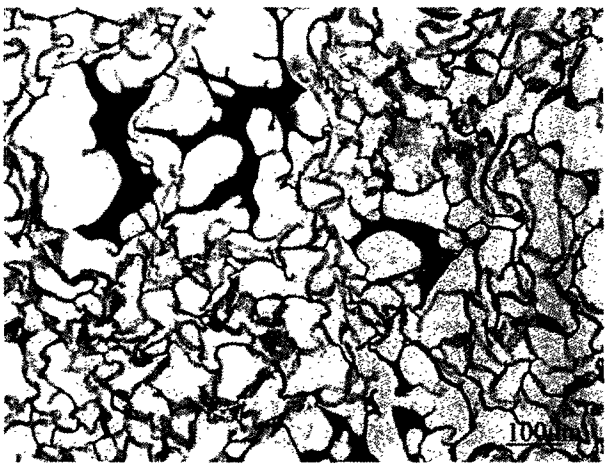

Figure 13 DHT-treated type I collagen-GAG scaffold after 3 weeks in culture. Scaffold was not prehydrated. H&E; 100X.

4.3 Scaffold Contraction

A two factor ANOVA analysis and Fisher's LSPD are used to determine the effect of cell-seeding on scaffold contraction. Cell-seeded scaffolds were found to have a significantly smaller mean scaffold diameter compared to unseeded controls ($p < 0.0001$; Power = 1) (**Figure 14**). This difference was also significant at every time point except during the initial seeding period (0 days). Mean measured diameter for 19-day fetal cell-seeded scaffold was 5.3±1.7mm and 6.1±1.0mm for unseeded controls. Mean scaffold contraction was 34.0% and 23.7% for 19-day fetal cell-seeded and unseeded collagen scaffold respectively. Scaffold contraction was not found to be significant for 20-day fetal rat lung cells ($p = 0.5437$). Mean scaffold contraction was 9.9% and 13.2% for unseeded controls and 20-day fetal cell-seeded scaffold respectively. Mean scaffold diameter measured for 20-days gestation fetal cell-seeded scaffold was 6.6±0.7mm and 6.3±0.9mm for unseeded controls. Scaffold contraction was highly significant ($p < 0.0001$) for 2-day neonatal cell-seeded scaffold compared to unseeded controls. Mean diameter of neonatal cell-seeded and control scaffolds were 4.92±2.4mm and 6.2±0.35mm respectively. At the end of three weeks, 16-day, 19-day, 20-day fetal, and 2 days neonatal cell-seeded scaffolds had contracted to 68%, 42%, 73%, and 25% of original scaffold diameter respectively compared to 72% contraction of unseeded scaffolds (**Figure 15**). Therefore, cell-mediated contraction at the end of three weeks in culture for 16-day, 19-day fetal and 2 days neonatal cell-seeded scaffolds were 4%, 30%, and 47% respectively while there was no cell-mediated contraction in the 20-day fetal cell-seeded study.

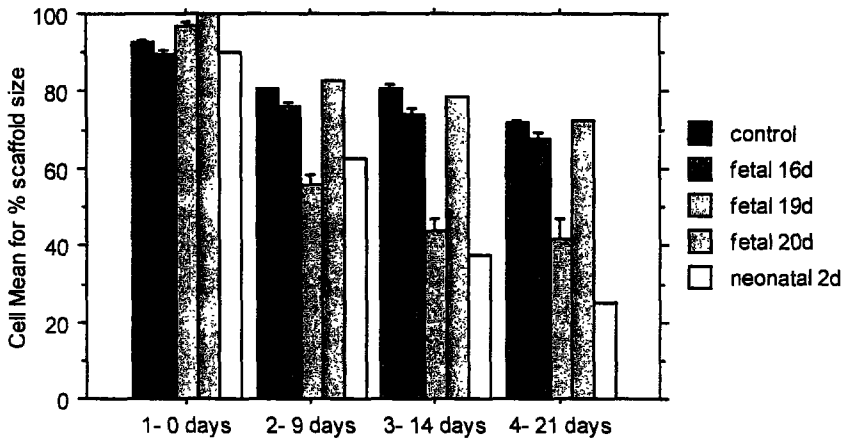

Figure 14 Bar plot of percent contraction of original scaffold diameter of unseeded, 16-days, 19-days, 20-days gestation, and 2-days neonatal cell-seeded scaffolds after 0, 9, 14, and 21 days in culture. Error bars represent one standard deviation with a 95% confidence interval. $N_{control} = 42$, $N_{16\text{-}days} = 12$, $N_{19\text{-}days} = 35$, $N_{20\text{-}days} = 34$, $N_{2\text{-}days} = 12$.

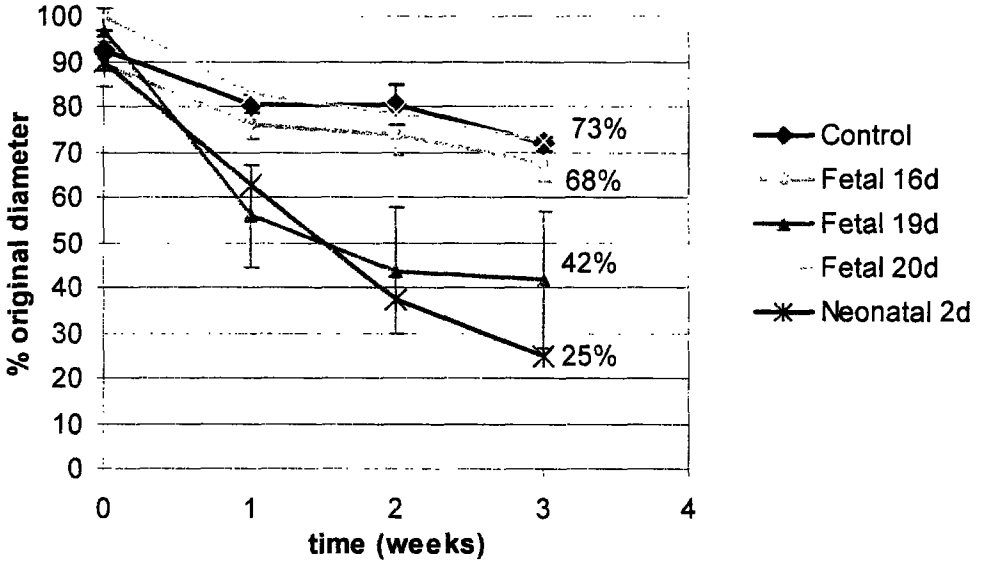

Figure 15 Line plot of scaffold contraction for control, 16-day, 19-day, 20-day fetal and 2 days neonatal rats seeded in DHT-treated type I collagen-GAG matrix cultures up to 3 weeks. Scaffold contraction for control at 3 weeks was 72%.

4.4 Mice Lung

The photomicrographs below are tissue sections from 10-day-old mice lung. Sections are stained using hematoxylin and eosin stain, elastin stain, anti-smooth muscle actin antibody immunostain, and anti-cytokeratin antibody immunostain. The respiratory unit of the lung can be seen in **Figure 16**: alveolar ducts open into alveolar sacs and alveoli. The respiratory bronchiole tissue and pseudostratified columnar epithelium characteristic of the respiratory system is seen in **Figures 17-19**. The lung tissue is rich in elastin (**Figure 18**) and actin (**Figure 17**), particularly the respiratory bronchiole tissue. Mice lungs were negative for monoclonal mouse anti-cytokeratin antibody (**Figure 19**).

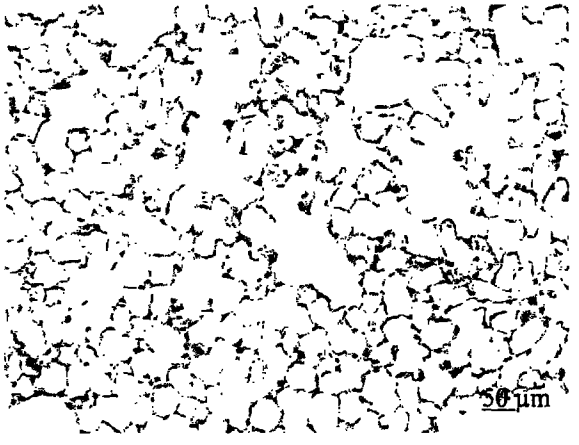

Figure 16 Photomicrograph of lung section from 10-day-old mice. H&E; 200X.

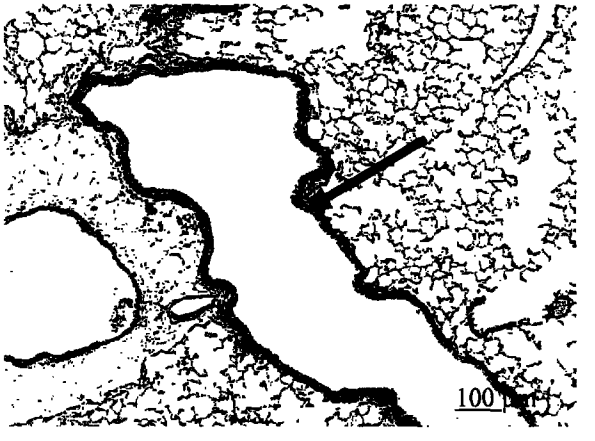

Figure 17 Photomicrograph of lung section from 10-day-old mice. The red represents positive staining for smooth muscle-actin (arrow). SMA; 100X.

Figure 18 Photomicrograph of lung section from 10-day-old mice where elastin tissue is stained black. Positive staining can be seen in the alveolar cells. Elastin; 200X.

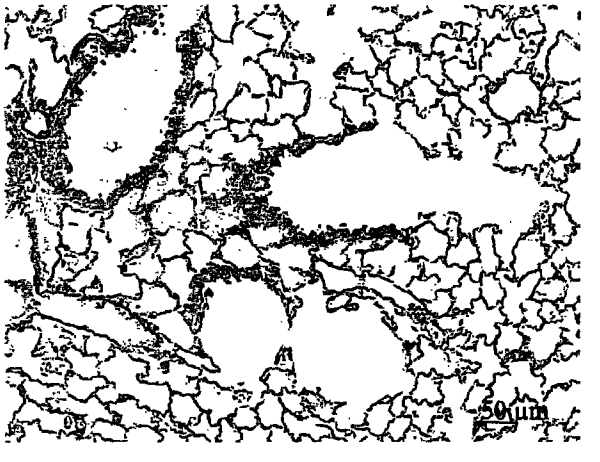

Figure 19 Photomicrograph of lung section from 10-day-old mice stained for cytokeratin. Positive staining can be seen in the alveolar cells. Cytokeratin; 200X.

4.5 Mice study

In both studies conducted, very few cells were observed by H&E staining. In the first study, 326 million cells were obtained from 13 mice or roughly 25 million cells/mouse. However, this large number reflects all the cells in the sample including a lot of red blood cells. Unfortunately, the cell counting method does not differentiate between different types of cells. These cells were frozen for a week before cell-seeding. During the time of seeding, only 120 million cells remained viable. In the second study, we attempted to isolate alveolar epithelial cells in the cell population and remove fibroblasts and other cells by differential adherence. Using this method, 23 million cells were obtained from 11 mice or 2.09×10^6cells/mouse. Samples of the cells and matrix were stained with H&E and examined using light microscopy. The cells did not appear to adhere to the collagen matrix. The few cells that were found within the matrix were concentrated at the scaffold perimeter and poor viability was observed. These observations were true for both DHT-treated and EDAC-treated matrices. No significant difference was found between the two types of matrices.

4.6 Fetal Rat Lung

Lung tissue from 19-days-gestation fetal rats are sectioned and stained with hematoxylin & eosin (**Figure 20**) and elastin stain (**Figure 21**). The lung tissues of the fetal rats are very rich in cells whereas very little extracellular matrix tissue is observed at this stage. The cells appear in morphology similar to cuboidal type II alveolar cells.

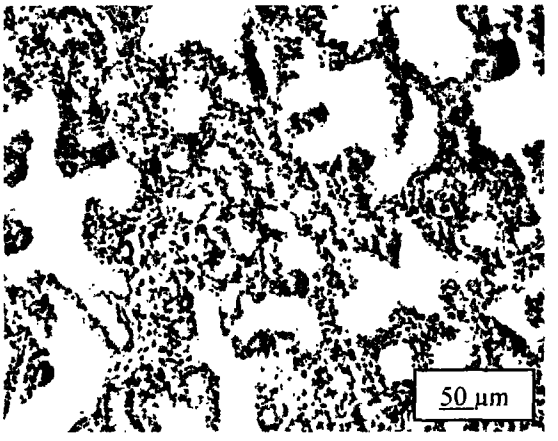

Figure 20 Photomicrograph of 19-days-gestation fetal rat lung. H&E; 200X.

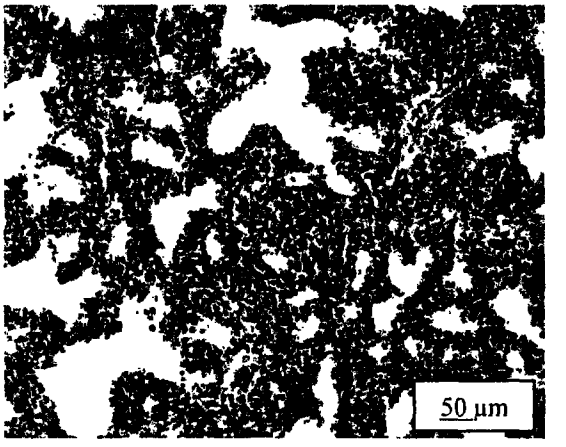

Figure 21 Photomicrograph of 19-days-gestation fetal rat lung. Elastin stain; 200X.

4.7 Neonatal Study

In this study, alveolar-like structures were not present. After one week in culture, most of the cells were located peripherally with fewer cells at the center of the scaffold (**Figure 22**). Cells appeared stratified or pseudostratified in morphology at the perimeter of the scaffold while cells within the scaffold remained cuboidal. After two weeks in culture, more collagen secretions were seen through the collagen matrix and the cells at the perimeter became more attenuated. Within the matrix, cells remained cuboidal, undergoing growth and appear larger in size (**Figure 23**). After three weeks in culture, the cells had developed into a stratified cuboidal epithelium (**Figure 24**). The samples were fed media in a static culture. A cell-gradient of viability can be seen in **Figure 25**, where the media and oxygen are diffusion-limited to the perimeter of the scaffold. Cell apoptosis, cytoplasm, and nuclear fragmentation are observed within the matrix.

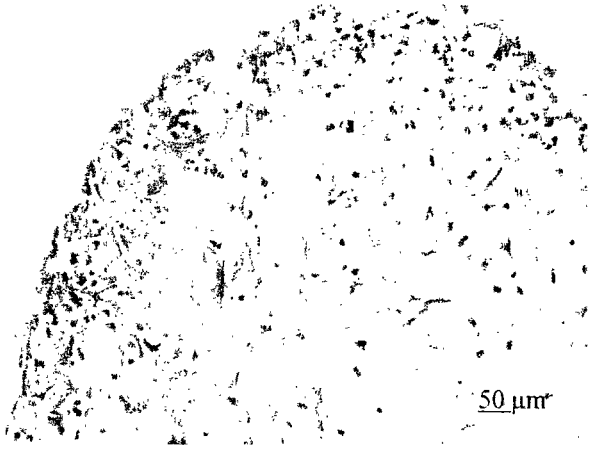

Figure 22 Photomicrograph of perimeter of neonatal cell-seeded scaffold after 1 week in culture. H&E; 200X

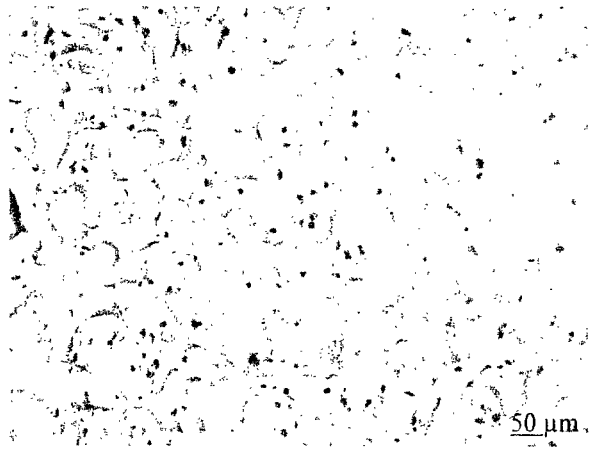

Figure 23 Photomicrograph of center of cell-seeded scaffold after 2 weeks in culture. H&E; 200X.

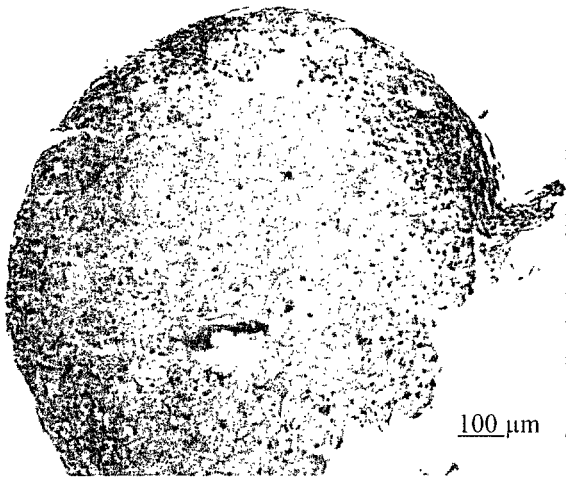

Figure 24 Photomicrograph of cell-seeded DHT-treated scaffold after 3 weeks in culture. H&E; 100X

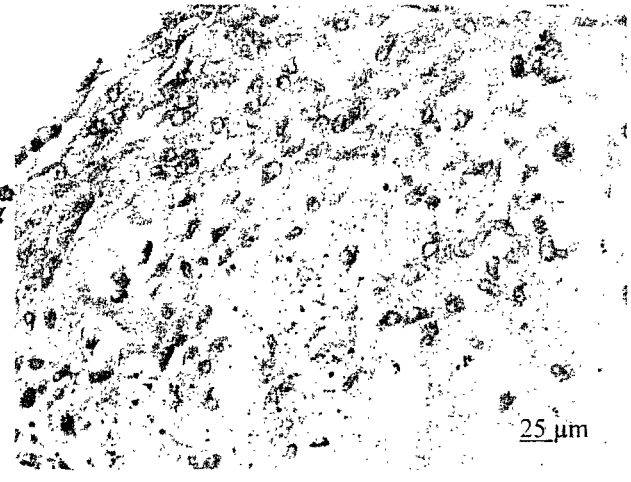

Figure 25 Photomicrograph of cell viability gradient seen in scaffold after 3 weeks in culture. H&E; 400X.

4.8 16 days gestation fetal study

No structural formation was found in the 16-days gestation fetal study. A total of $18.2x10^6$cells was obtained from 12 fetuses with a cell viability of 94.6%. The cell-seeding density used in the study was $2.3x10^6$cells/matrix. Both DHT cross-linked and EDAC cross-linked type I collagen-GAG matrices were used.

After 1 week in culture, the cells in the EDAC-treated scaffolds were largely located in the perimeter. Cell morphology was attenuated at the perimeter but round and cuboidal at the center. However, only a very sparse number of cells were observed in the scaffold center and the beginning of scaffold degradation can be seen at the center.

On the other hand, after 1 week in culture, the cells seeded in DHT-treated scaffolds were uniformly distributed along with many red blood cells throughout the matrix (**Figure 26**). Contraction was also clearly evident and cells stain positively for smooth-muscle actin antibody (**Figure 27**), but no actual alveolar-like structure is present.

After 2 weeks in culture, the cells seeded in the EDAC-treated scaffolds are observed mostly on one side of the matrix within 1mm thickness (**Figure 28**), while cells seeded in the DHT-treated scaffolds mostly contain a lot of red blood cells with few other cells (**Figure 30**).

After 3 weeks in culture, most of the cells seeded in EDAC-treated (**Figure 29**) and DHT-treated (**Figure 31**) scaffolds have undergone apoptosis and only cell debris and cytoplasm remain.

Figure 26 DHT-treated matrix seeded with 16-days gestation fetal lung cells after 1 week in culture. H&E stain; 400X.

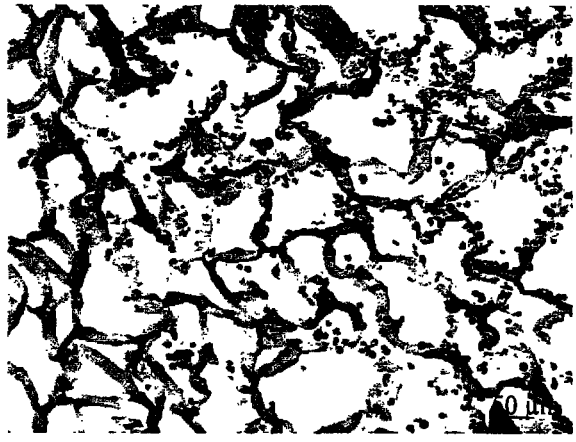

Figure 27 DHT-treated matrix seeded with 16-days gestation fetal lung cells after 1 week in culture. Cells have positive staining for SMA (arrow). SMA stain; 200X.

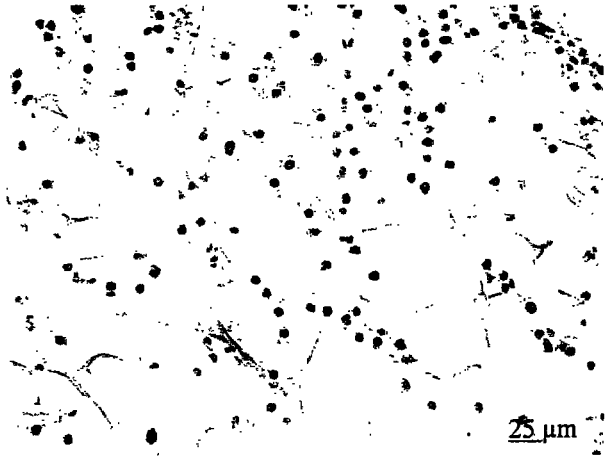

Figure 28 Photomicrograph of 16-days-gestation fetal rats seeded in an EDAC-treated collagen matrix after 2 weeks in culture. H&E; 400X.

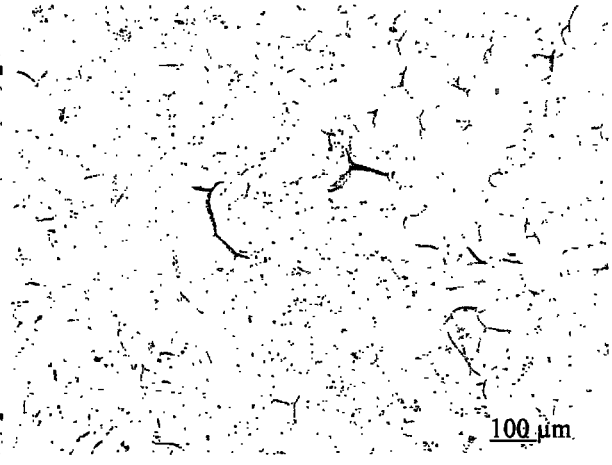

Figure 29 Photomicrograph of 16-days-gestation fetal rats seeded in an EDAC-treated matrix after 3 weeks in culture. H&E; 100X.

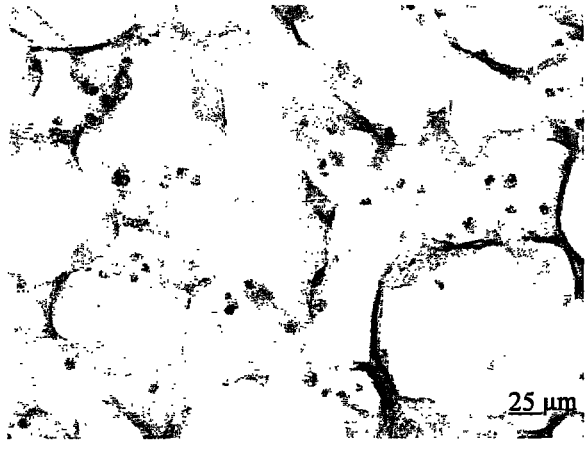

Figure 30 Photomicrograph of cell-seeded DHT-treated scaffold after 2 weeks in culture. H&E; 400X.

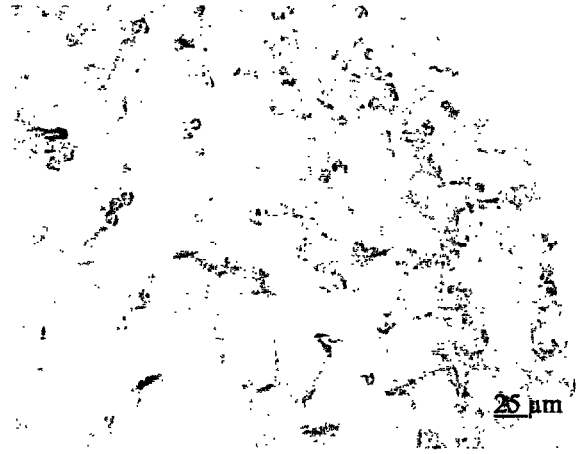

Figure 31 Photomicrograph of cell-seeded DHT-treated scaffold after 3 weeks in culture. H&E; 400X.

4.9 20 days gestation fetal study

In the study performed using 20-days gestation fetal cells, no structural formation was found. The cells were immunopositive for anti-cytokeratin antibody (**Figure 32, 33**) but negative for smooth-muscle actin antibody (**Figure 34**). Even after 1 week in culture, loss of nuclei can be seen (**Figure 35**). By 3 weeks in culture, all cells had undergone apoptosis (**Figure 34**).

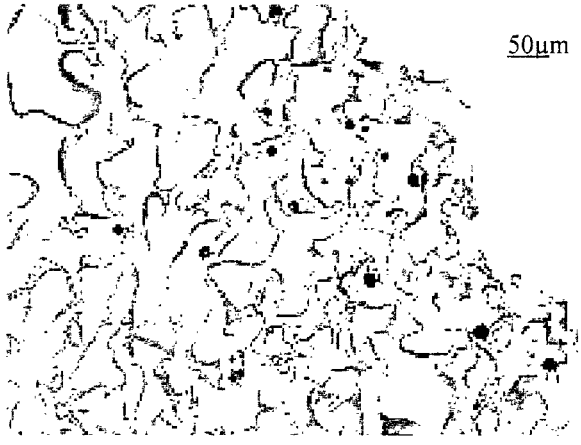

Figure 32 Photomicrograph of 20-days gestation fetal lung cells seeded in DHT-treated collagen matrix after 1 week in culture. Cytokeratin stain; 200X

Figure 33 Photomicrograph of 20-days gestation fetal lung cells seeded in DHT-treated collagen matrix after 3 weeks in culture. Clear positive staining for cytokeratin can be seen . Cytokeratin; 100X.

Figure 34 Photomicrograph of 20-days gestation fetal lung cells after 3 weeks in culture. SMA; 100X.

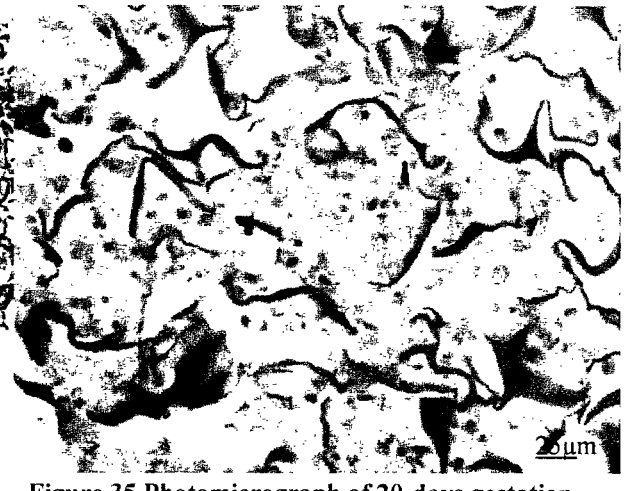

Figure 35 Photomicrograph of 20-days gestation fetal lung cells seeded in matrix after 1 week in culture. H&E; 400X.

4.10 19 days gestation fetal study

In the study performed with 19-days-gestation fetal rat cells, alveolar-like structural formation was not found until after 2 weeks in culture. After 2 days post-seeding, cells appeared uniformly monodispersed throughout a porous, well-intact collagen-GAG matrix (**Figure 36**). After 2 weeks in culture, alveolar-like structures were found localized at the edges and perimeter of the scaffolds where cell density was higher (**Figure 37**). Some but fewer ALS were located in the middle of the matrix (**Figure 37**). Structures found after 2 week in culture are alveolar-like for the following reasons: 1) the cells comprising the structures are cuboidal with apical-basal polarity and microvilli on their apical surface (**Figure 37**) resembling type II alveolar cells found in the alveoli of the lung *in vivo,* 2) the structures abut the collagen matrices basally and form a central lumen apically basally as observed in the tissue section stained with Masson Trichrome (**Figure 39**) and is similar to the architecture of the normal *in vivo* alveoli, 3) alveolar-like structures are surrounded by tissue positive for smooth-muscle actin (**Figures 42-43**) which is also found in the adult lung tissue (**Figure 17**), 4) cells appear to secrete pulmonary surfactant characteristic of type II alveolar cells (**Figure 40**), 5) the cells that compose the structures contain cytokeratin, an intermediate filament only present in alveolar cells in the lungs (**Figure 44**), and 6) elastin is abundantly present in the structures (**Figure 45**) as was also found in the adult lung tissue (**Figure 18**). These alveolar-like structures were maintained up to 3 weeks in culture (**Figure 38, 40, 41**).

When cells were seeded onto dry matrices, no structural formation was observed. After 2 days, cells were distributed non-uniformly with a concentrated aliquot of cells in the middle of the matrix where it had been initially seeded (**Figure 46**). Cells were viable after 2 weeks in culture but no alveolar-like formation was found (**Figure 47**). Minimal interaction was observed between the collagen matrix and the cells even after 3 weeks in culture (**Figure 48**). This is also verified by the lack of scaffold contraction in culture after 3 weeks (results not shown). In a photomicrograph of the thickness of the cell-seeded scaffold after 3 weeks in culture, cells remained seeded on one side of the matrix and minimal cell migration and activity was observed (**Figure 49**).

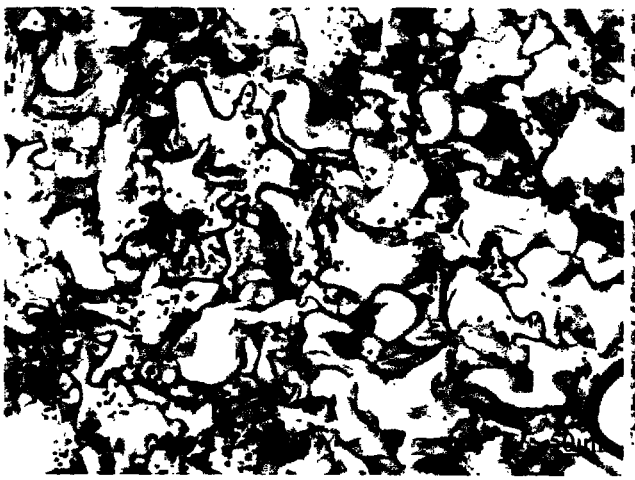

Figure 36 Photomicrograph of 19-days gestation cell-seeded scaffold after 2 days in culture. The cells are monodispersed within the collagen matrix. H&E stain; X200.

Figure 37 Photomicrograph of 19-days gestation cell-seeded scaffold after 2 weeks in culture. Two arrows each point to alveolar-like structures. Pulmonary surfactant secreted by the cells can also be seen. H&E stain; X200.

Figure 38 Photomicrograph of cell-seeded scaffold after 3 weeks in culture. The arrow points to a growing alveolar-like structure. H&E stain; X200.

Figure 39 Photomicrograph of cell-seeded scaffold after 2 weeks in culture. Masson trichrome stain is a three dye stain that stains collagen blue, nuclei black, and cytoplasm red; X200. The arrow points to an alveolar-like structure.

Figure 40 Photomicrograph of cell-seeded scaffold after 3 weeks in culture. Arrow points to surfactant secretion. H&E; 200X.

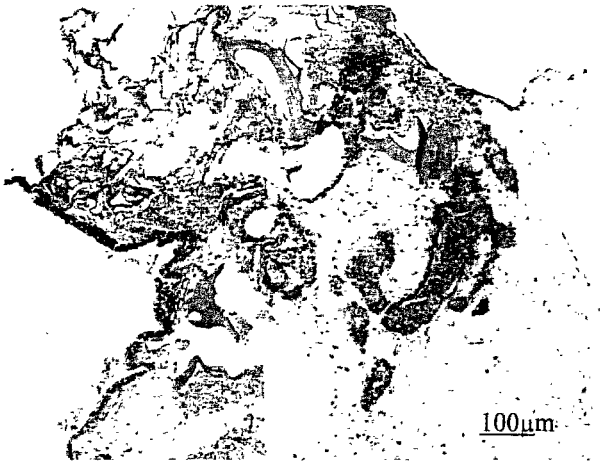

Figure 41 Photomicrograph of cell-seeded scaffold after 3 weeks in culture. H&E; 100X.

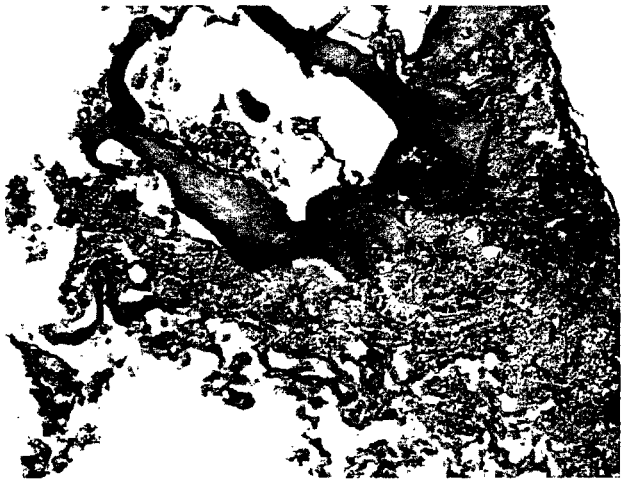

Figure 42 Photomicrograph of ALS with positive SMA stain around structure. SMA; 200X.

Figure 43 Photomicrograph of ALS surrounded with positive SMA (arrow). SMA; 400X.

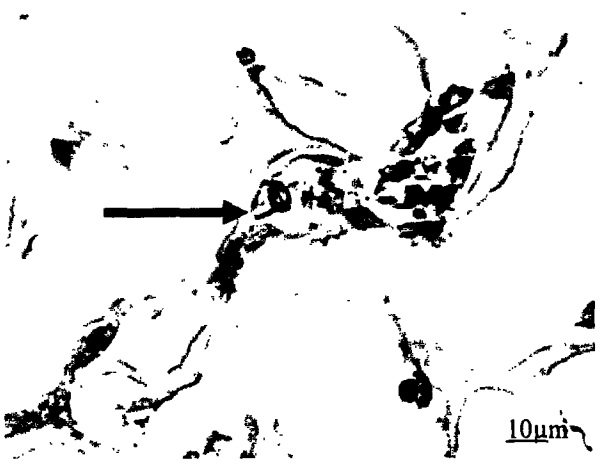

Figure 44 Photomicrograph of type II alveolar cells with positive cytokeratin intermediate filament staining in cytoplasm(arrow). Cytokeratin; 1000X.

Figure 45 Photomicrograph of ALS stained for elastin after 2 weeks in culture. Elastin; 100X.

Figure 46 Photomicrograph of 19-days gestation cell-seeded scaffold after 2 days in culture. H&E; 100X.

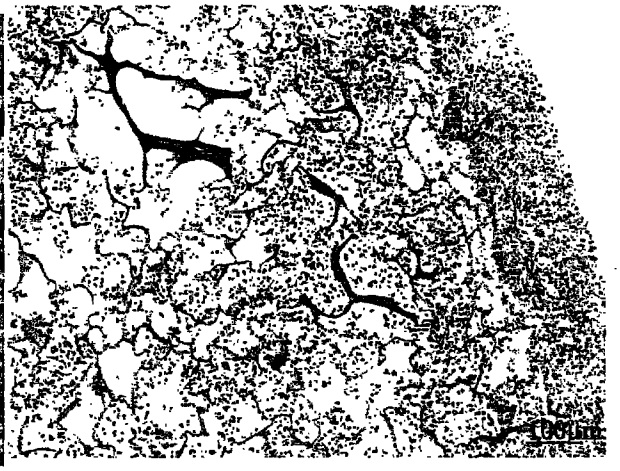

Figure 47 Photomicrograph of 19-days gestation cell-seeded scaffold after 2 weeks in culture. H&E; 100X.

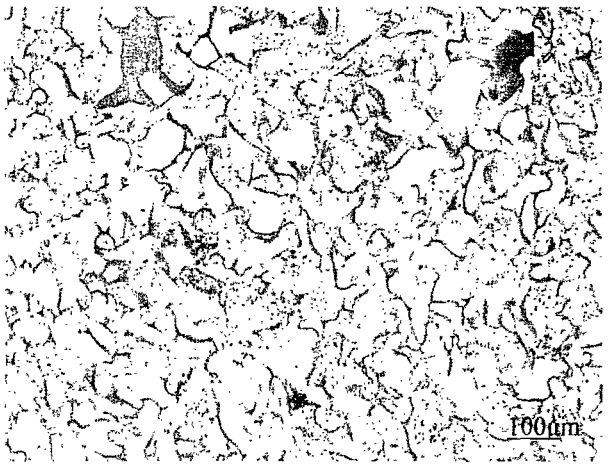

Figure 48 Photomicrograph of 19-days gestation cell-seeded scaffold after 3 weeks in culture. H&E; 100X.

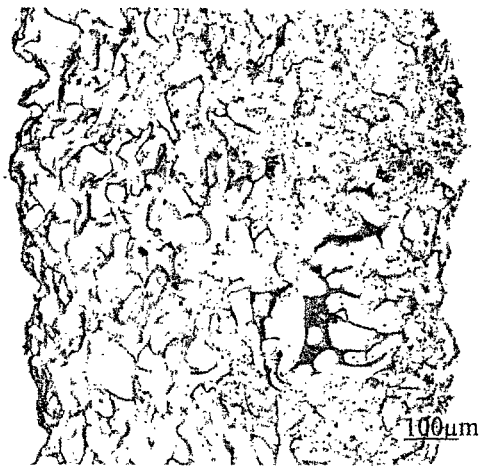

Figure 49 Photomicrograph of scaffold thickness of 19-days gestation cell-seeded scaffold after 3 weeks in culture. H&E; 100X.

4.11 DNA Assay

Results from the pico-green DNA assay show a decreasing amount of DNA and a decreasing cell number in cultures with time. Results for the cell number (mean±SD) in culture for 19-days gestation and 20-days gestation fetal studies are shown below.

Figure 50 Bar graph (mean ± st. dev) of 19-days gestation cell number at 2, 14, and 21 days in culture. $N_{2\ days} = 6$, $N_{14\ days} = 5$, $N_{21\ days} = 4$.

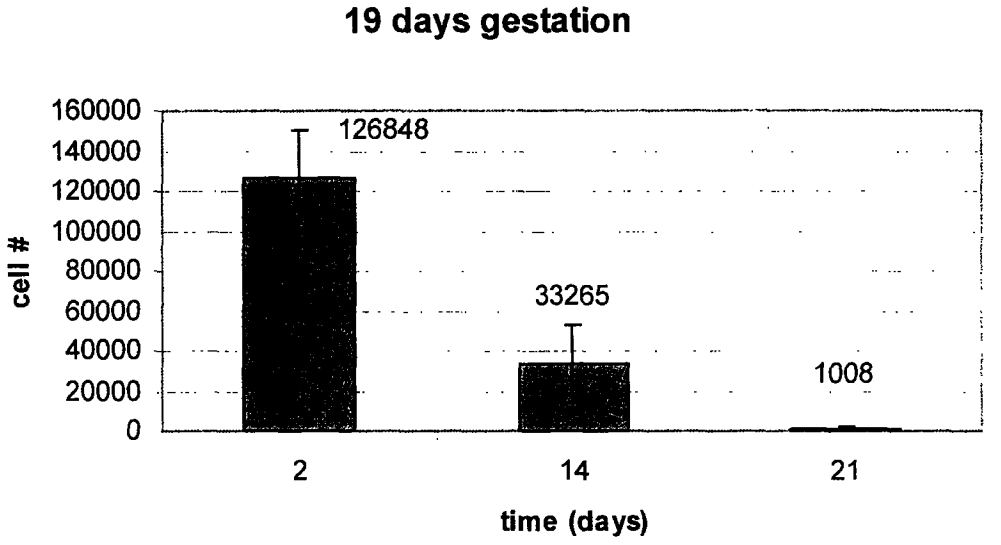

Figure 51 Bar graph (mean ± st. dev) of 20-days gestation cell number at 2, 14, 21 days in culture. $N_{2\text{-}days} = 3$, $N_{10\text{-}days} = 5$, $N_{14\text{-}days} = 5$, $N_{21\text{-}days} = 4$.

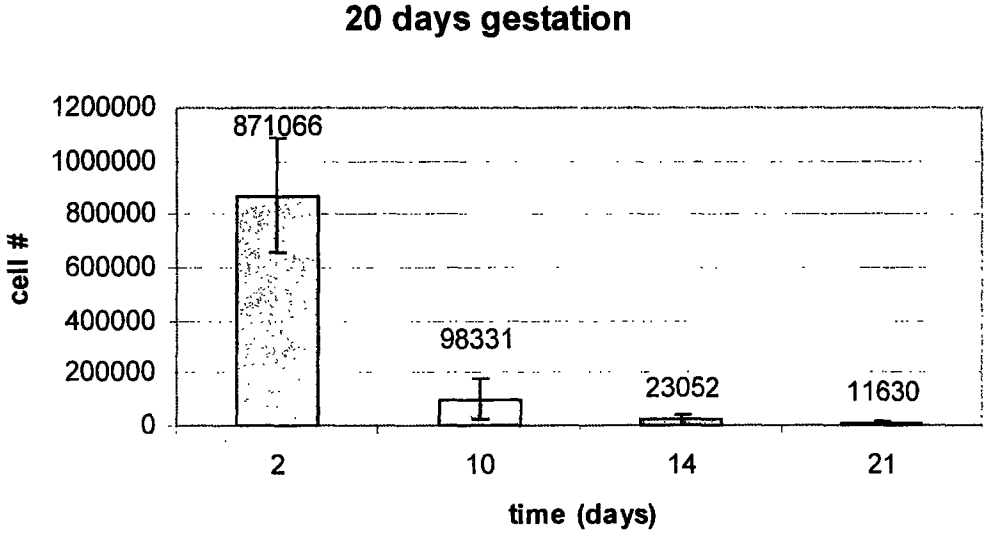

4.12 Collagen-GAG Assay

From the collagen-GAG assay performed, very little GAG was produced in the cultures.

4.13 Quantification of Alveolar-like Structures

Only alveolar-like structures were found in the DHT-treated type I collagen-GAG scaffolds seeded with 19-days gestation fetal rat cells. No alveolar-like structures were found up to 1 week in cultures. Alveolar-like structures were found in cultures at 2 weeks and 3 weeks. An ANOVA analysis of the ALS shows no significant difference in the size of the structures between week 2 and week 3. The average ALS at 2 weeks and 3 weeks was 52.5±24.9μm and 60.2±33.2μm (mean ± SD) (**Figure 52**). In the samples analyzed, a total of 30 ALS and 28 ALS were found at 2 weeks and 3 weeks. A Fisher's PLSD analysis for average ALS found no significant difference between week 2 and 3 ($p=0.3969$). Average number of ALS found was 10.4/mm^2 and 9.8/mm^2 after 2 weeks and 3 weeks in culture respectively. The largest structures found after 2 weeks and 3 weeks in culture were 130μm and 160μm in diameter respectively.

The form factor is an aspect ratio that defines the shape of the alveolar-like structures. A perfectly circular ALS has a form factor of 1 while elliptical structures and deviations from round structures are between 0 and 1 (**Figure 53**). The average form factors after 2 weeks and 3 weeks in culture were 0.7±0.2 and 0.6± 0.2.

Figure 52 Bar graph of average size of alveolar-like structure after 2 weeks and 3 weeks in culture. No structures were found in scaffolds after 2 days in culture. Study was terminated after 3 weeks. $N_{2\text{-weeks}}= 30$, $N_{3\text{-weeks}}= 28$.

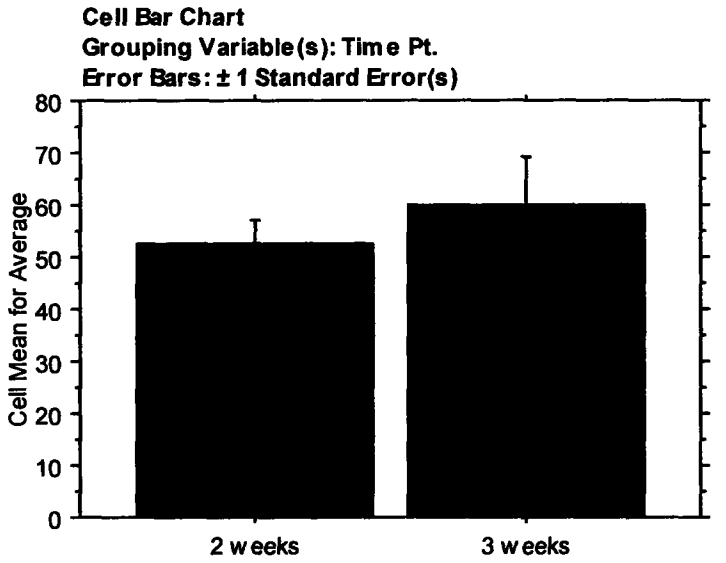

Figure 53 Form Factor calculated for alveolar-like structures after 2 weeks and 3 weeks in culture. A slope of 1 indicated a round structure.

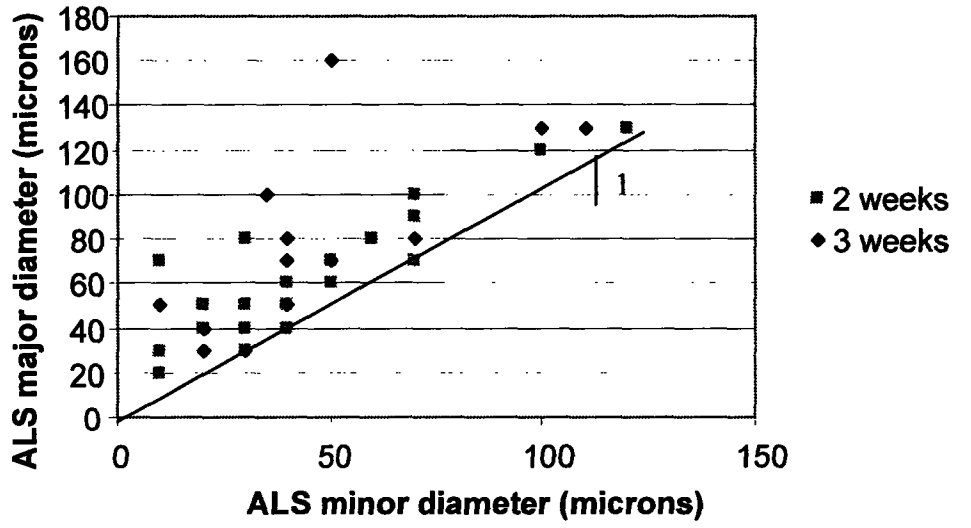

Chapter 5 Discussion & Conclusion

5.1 Development of a cell isolation procedure whereby cells are enzymatically dissociated from fetal and neonatal rat lungs while maintaining cell surface receptors which are critical in regeneration of lung structures.

A careful cell isolation procedure is critical to the maintenance of cell surface receptors needed for regeneration of lung structures. Enzymatic dissociation of lung tissue is performed in a series of steps and filtered through different pore-size meshes to obtain a final monodispersed cell suspension. Cells are chilled on ice to slow down cellular metabolism during lung cell isolation.

The cell-to-cell interactions involved in the reaggregation process and structural formation require cell membrane bound macromolecular components similar to those described in the embryo cells. Proteolytic treatment disrupts specific cell-ligand components, and if reaggregation is to occur, these structures must reform. Incubation of cell pellet before cell-seeding is believed to allow resynthesis and the formation of cell surface components.

The use of primary cells is also important to lung tissue regeneration. The lung is a complex organ composed of a diverse cell population. Type II cells plated on tissue culture plastic dedifferentiate and inhibit the formation of lung structures. In studies performed by previous investigators, the tissue digestion and cell isolation procedure were performed to obtain a high yield of type II alveolar cells and alveolar-like structures were also observed. In all cases however, the use of a primary cell population was needed for *in vitro* formation of alveolar-like structures.

The procedure developed in this study maintains the surface receptors of 19-days gestation type II alveolar cells and promotes the formation of alveolar-like structures in our *in vitro* system.

5.2 Identification of fetal and neonatal lung cell behavior differences using histological analysis.

From analysis of the studies performed, differences have been observed between fetal and neonatal lung cell behavior. We have found no alveolar-like formation with neonatal lung cells from Sprague-Dawley rats or mice. In addition, alveolar-like formation was not found using lung cells from fetal Sprague-Dawley rats at 16-days gestation and 20-days gestation. Alveolar-like structural formation was only found using a cell source from 19-days gestation fetal rat cells. Results from this study suggest that alveolar formation in lungs occur at 19-days gestation when cultured in our *in vitro* system. It also appears that only at 19-days gestation do cells express the necessary cell receptors for reaggregation into alveolar-like structures *in vitro*. These results differ from work done by other investigators where structural formation was observed with different gestation fetal [12] and adult rat lung cells [10]. Further investigation will have to be done to determine whether differences are due to our *in vitro* system or to variances in cell isolation and culture methods.

Other significant differences found between fetal and neonatal lung cells are smooth muscle actin expression and collagen-GAG matrix contraction. The presence of smooth muscle actin is found in greater amounts in neonatal cells compared to fetal cells and correlate with differences in scaffold contraction observed over time. Samples seeded with neonatal lung cells were found to contract significantly more over time compared to scaffolds seeded with fetal lung cells. This phenomena is analogous to the change seen in wound healing process from skin regeneration in the fetus to fibrous scar formation in the adult described by Yannas [26].

Cell-matrix interactions dominate in the neonatal cell culture system. In fetal cell culture system, cell-cell interactions dominate. The presence of alveolar-like structures is only found in fetal cells while pulmonary surfactant synthesis is found in both fetal and neonatal alveolar cells. The difference in cell behavior between neonatal and fetal lung cells can be explained by a difference in cell surface receptor expression. This is supported by observed differences in lung architecture between the fetal lung and neonatal lung. The respiratory portion of the fetal lung comprises almost entirely of alveolar cells while in the neonates and adults, all the alveolar cells underlie an

extracellular matrix. The extracellular matrix components are partially secreted by the alveolar cells. This correlates with completion of alveolar formation which occurs during late gestation after epithelial cells differentiate into type I and type II alveolar cells.

5.3 Investigation of the effects of selected scaffold design variables on lung tissue regeneration in our *in vitro* system.

The type I collagen-GAG scaffold is an appropriate extracellular matrix analog for lung tissue regeneration. Collagen is found abundantly in the native lung and functions to provide support. In the alveolus and small airways, collagen is found in the interstitium and basement membrane. Type I collagen constitutes a large portion of the collagen found in the lung and thus provides most of the lung tissue support. In the lung, type I alveolar cells predominantly overlie capillaries where the matrix is mostly type IV collagen and laminin, whereas type II alveolar cells are usually found in corners where there is an additional matrix component of type I collagen. The lung cells that have been found to secrete type I collagen are largely classified as mesenchymal cells. These cells have similar morphology and include fibroblasts, interstitial cells, contractile cells, and pericytes. The collagen scaffold lacks type III collagen also known as fetal lung named after its finding at higher amounts in younger animals. Type IV collagen is the primary collagen found in basement membranes and thus believed to anchor epithelial and endothelial cells. Since our study only has type I collagen, we only observe type II alveolar cells. Type I alveolar cells are not observed due to the lack of necessary matrix components such as type IV collagen. Type II cells are also not observed to differentiated into type I cells at the end of 3 weeks in culture. A longer culture period can be performed to determine whether type II cells differentiate to type I cells over a longer time.

In this study, dehydrothermally (DHT) cross-linked type I collagen-GAG matrices were used which are structurally similar to the Gelfoam sponges previously used except suitable for tissue engineering. The collagen-GAG matrix should produce an environment which facilitates cell-cell contact and provide adequate media supply making it conducive to aggregate formation. The sponge-like structure with its random

trabeculae is expected to promote the formation of numerous individual aggregate elements by compartmentalizing the cell inoculum without obstructing cell movement. The main advantage of using a three-dimensional lattice culture is so that the cells can easily migrate through the flexible matrix and find their nutrients inside the collagen scaffold both by their apical and basal surfaces. The process of alveolar-like formation appears to be closely dependent on the fact that both basal and apical sides of the epithelial cells are covered by collagen. The process of tubule formation may be due to either the physical properties of the lattice which possess a loose and flexible fibrillar structure or secondary to the interaction of the cell surface integrin receptors with collagen [27].

EDAC cross-linked scaffolds did not allow reaggregation of cells into ALS. Chemically cross-linking scaffolds prevented cells to contract scaffold and aggregate together. EDAC cross-linked scaffolds also degrade at a slower rate compared to DHT cross-linked scaffolds. Formation of ALS appears to depend on cell contraction of scaffold, followed by degradation of matrix, and formation into aggregates.

When matrices were not prehydrated before cell-seeding, structural formation was also not observed. In fact, there was minimal activity observed due to the inability of the cells to infiltrate into the matrix and adhere onto the collagen matrix surface. Cells cannot proliferate, migrate, and synthesize without adhesion to the extracellular matrix via cell-surface molecules known as integrins. It appears from the study that cell-cell interactions are also prohibited by the lack of cell-matrix interactions. Therefore, no aggregation or alveolar-like formations were observed even after three weeks. After three weeks in culture, the cells were still poorly distributed and no cells were evident on the bottom portion of the matrix. From this study, we confirm that both cell-matrix and cell-cell interactions appear critical for the formation of alveolar-like structures and that the process of prehydrating the matrix before cell-seeding allows the matrix to swell and allows cells to migrate into the matrix and adhere onto the matrix surfaces. It seems that while cell-cell interactions are critical to the formation of alveolar-like structures, cell-matrix interactions play a key role preceding this event.

Alveolar-like structural formation was found using collagen-GAG scaffolds of mean pore size 95.9μm (dry). This pore size was large enough to allow cell migration

into scaffold and aggregation into alveolar-like structures. However, we have found that scaffold pore size does not appear to have a significant effect on the formation of alveolar-like structures. It is only important that the pore size be large enough to allow cells migration into scaffold and nutrients diffusion through scaffold.

5.4 Investigation of lung cell behavior revealed as the cells interact with an analog of the extracellular matrix.

Results from the studies carried out also reveal that cell source and age may play an important role in the formation of alveolar-like structures. Structural formation was not found using neonatal cells from mice or rats nor from 16-days or 20-days gestation fetal rat lung cells. Structural formation was only found when collagen-GAG matrices were cultured with 19-days gestation fetal lung cells. Our results differ from results concluded by Sorokin who found that formation of alveolar-like structures depended on time spent in culture rather than with gestational age of cells used. It was concluded that cells of different gestational age differentiated at similar rates when cultured *in vitro* [28].

There are several explanations for why there were no structural formations in the study using lung cells from mice. One possibility is that lung cells from mice have different surface receptors from rats and do not recognize the ligands on type I collagen matrix surfaces. This is supported by the finding that there was minimal interaction of the cells with the matrix. However, there was also very little cell-cell interaction found. Another possibility is that cell surfaces were damaged during the isolation and freezing procedure. A more likely possibility is that cells had dedifferentiated after plating. It appears that the use of primary cells is critical for structural formation. The effect of lung cells from different species of animals (mice vs. rats) in the formation of lung structures remains unclear and will have to be further investigated.

From the results found through the histological studies and DNA assay, cells are not proliferating over time. Even in the presence of alveolar-like structural formation and maintenance of structures up to 3 weeks, the cell number in our cultures decreased over the 3 weeks in our study. Interestingly, the ALS observed were localized in their area of formation. Most structures were found peripherally of the matrix and in the center of the matrix where there was massive degradation of the matrix. Only a few structures were

found deeply embedded within the matrix. These observations suggest that factors such as oxygen and specific matrix architecture determine not only alveolar-like structural formation but also cell apoptosis. From our results, it appears that while structures were maintained over three weeks, the remaining cells in culture underwent apoptosis over time. It is possible that alveolar cells may be programmed for alveolar formation so that cells not participating in alveolar formation undergo programmed death. The formation of structures at sites of maximum oxygen and nutrient exchange mimics the *in vivo* lung architecture where carbon dioxide and oxygen gas exchange occurs continuously through the tissue.

Contractile properties exhibited by the type II alveolar cells and the contraction of the substratum is believed to promote the formation of the alveolar-like structures. Contraction of the collagen-GAG scaffold allows type II cells to remain cuboidal in shape rather than attenuating and dedifferentiation and thus represents an environment similar to one *in vivo.* When type II cells are cultured on tissue culture plastic in the presence of 5 – 10% FBS, cells undergo extensive morphological changes which include lost of cuboidal appearance, cell flattening, decrease in size and number of lamellar bodies, and dramatic decrease in surfactant synthesis. In a three-dimensional collagen-GAG scaffold, type II cells appear to maintain morphologic characteristics of type II cells *in vivo* – i.e. apical-basal polarity, basal lamina secreted and formed, and well-developed junctional complexes.

5.5 Theory for the formation of alveolar-like structures

Several theories for the formation of alveolar-like structures can be postulated from analysis of the results in this thesis. An alveolar-like structure is defined in this study as a structure composed of cuboidal type II cells which attach onto the type I collagen-GAG matrix and form via intercellular junctional complexes into a structure with a central lumen resembling an alveolus. These structures may or may not have pulmonary surfactant secreted apically by the type II cells into the lumen.

The first theory for the formation of ALS is by spontaneous aggregation of structures. Cells attach via integrins to the type I collagen-GAG matrix and migrate through the pores forming cell-matrix interactions. Cells contract the scaffold exhibiting

smooth muscle-actin phenotype in order to form cell-cell interactions. This process is repeated over time resulting in the final formation of an alveolar-like structure composed of type II alveolar cells. Evidence that supports this theory includes our results for the correlation of cell-mediated contraction and ALS formation and the lack of ALS found when there was minimal contraction observed. Growth of structures and formation of more structures can occur by two possible ways. The first method is by division of a large tubular structure into smaller structures. This process is clearest in histological samples after 3 weeks in culture in scaffolds seeded with 19-days gestation fetal lung cells. Structures can initially form from a dense aliquot of type II alveolar cells. As cells undergo mitosis, growth, and apoptosis, this can result in the formation of tubular structures. Evidence in support of this theory is in the observation of cell apoptosis at the center of the alveolar-like structures. The second method is by addition of smaller structures into larger structures. It is unclear from examination of the fixed tissue sections the direction of growth. It is therefore just as likely that small alveolar-like structures coalesce together to form larger structures since there was no statistically significant difference found between the sizes of the ALS at 2 weeks and 3 weeks. In either case, the development of apical-basal polarity is evident by the secretion of pulmonary surfactant into the lumen of the alveolar-like structures from the apical surface of the epithelial cells.

Reconstruction of ALS from type II alveolar cells in a three-dimensional collagen matrix in culture occurs when the cell surfaces are in contact with the collagen matrix and in the appropriate physiological environment for cellular and structural differentiation. In other words, cell receptors play an essential role in the cellular differentiation and allow cells to communicate with the ECM towards structural differentiation. The findings here suggest that alveolar type II cells are self-differentiating cells and the type I collagen-GAG matrix supports the expression of differentiation. It appears that the maintenance of cell polarization in a thick three-dimensional substrate is important to surfactant synthesis, cell differentiation, phenotype preservation, and structural formation.

In conclusion, the formation of alveolar-like structures is found after 2 weeks in culture using 19-days gestation fetal rat lung cells and the ALS are maintained up to 3 weeks in our *in vitro* system. Several conclusions can also be inferred from the results of

studies performed using different cell sources and scaffold types. The results indicate that cell source appear to be critical to the formation of alveolar-like structures for our *in vitro* system. Structural formation was found only with 19-days gestation fetal rat lung cells. From our results, DHT cross-linked type I collagen-GAG scaffold is a suitable analog for lung tissue regeneration. In terms of the characteristics of the scaffold, it was found in the study that contraction of the scaffold was necessary in the formation of ALS. The characteristic pore size of the scaffold did not appear to affect lung tissue regeneration. The contraction of scaffold and expression of smooth muscle actin both play important roles in the fetal formation of alveolar-like structures. ALS was found in prehydrated DHT cross-linked scaffolds and not in EDAC cross-linked scaffolds or dry DHT cross-linked and therefore supports our belief that reaggregation of cells and the formation of cell-cell and cell-matrix interactions is critical in the formation of alveolar-like structures.

Chapter 6 Limitations and Future Work

6.1 Limitations

There are still many challenges to overcome in lung tissue engineering. The lung is an organ with a very unique and complicated architecture made up by a wide variety of highly differentiated cells. In fact, the lung parenchyma, airways, and pulmonary vasculature together have 40 different cell types. The unique architecture of each capillary vessel surrounded on both sides by one cell-thick epithelium needed to maximize efficiency of carbon dioxide-oxygen exchange is probably the greatest obstacle towards successful lung tissue engineering. This problem cannot be resolved until we know how to control and direct angiogenesis to create the intricate pulmonary vasculature.

In terms of limitations within this study, the results found only apply to a limited animal study performed *in vitro*. Results of this study need to be applied to larger animals and ultimately to the human lung *in vitro* and *in vivo*. Results found were also only applicable and limited to fetal and neonatal rat lung cells and no conclusions were made about the behavior of adult lung cells. All the results and conclusions were primarily based on analyses from histological sections.

The method described in this thesis for isolation of lung cells to maintain cell surface receptors and allow formation of alveolar-like structures may not be applicable to adult alveolar cells or to cells of different species. Investigation into a cell isolation procedure which maintains cell surface receptors in neonatal and adult lung cells is necessary for applications of this work clinically.

6.2 Future work

Type II alveolar cells should be verified by use of scanning electron microscopy to observe the osmiophilic lamellar bodies responsible for pulmonary surfactant production. Pulmonary surfactant secreted by type II alveolar cells can be used as a biochemical marker of differentiated type II cell phenotype. The major active component of the surfactant, dimpalmitoyl-phosphatidylcholine (PC), can be radioactively labeled through incorporation of [Me-^{3}He]choline into PC [11]. Immunocytochemical methods

can also be used to identify the surfactant proteins, SP-A, SP-B, SP-C. Alternatively, rat alveolar type II epithelial cells can also be identified using a tannic acid and polychrome stain [29]. Cell proliferation in culture can be examined using bromodeoxyuridine (BrdU) labeling reagent to investigate the behavior of cells.

The addition of growth factors and hormones into the media can enhance differentiation and growth of cells into histotypic structures or ALS. In previous work, the addition of various hormones was found to affect the branching morphogenesis of lung structures and the production of surfactant lipids. Differentiation and proliferation can be accelerated by treatment with dexamethasone [16] and thyroxine. Epidermal growth factor is also found to increase growth of structures. Others found transforming growth factor-beta to play a role in organizing cells into histotypic structures.

Future studies could also use both type I and type IV collagen in the scaffold as a better analog to the connective tissues and extracellular matrix of the lung. Only type I collagen was used as the ECM analog and for this reason, type I alveolar cells were not found in the *in vitro* system. The differentiation of type II cells into type I cells remains to be clarified. The use of laminin-coated matrices has also been found to promote retention of the cuboidal shape of type II cells and the role of laminin can be further investigated.

The bioreactor plays a very important role in successful lung tissue engineering and was not heavily explored. Future work could include the use of a bioreactor that mimics the environment in the lung which involves expansion and deflation of the lung parenchyma and variable oxygen and carbon dioxide diffusion through lung tissue.

Some initial work investigating the interaction between mesenchymal and epithelial cells has been done [30]; however, the use of cocultures has not been applied for lung tissue engineering. Results have been promising, particularly in the liver, in tissue engineering using cocultures of cells. The use of cocultures of mesenchymal cells and alveolar epithelial cells may result in a tissue more similar to the lung *in vivo*.

Just a few years ago, virtually no one thought lung tissue engineering was a possibility. Results from this thesis now verify the potential for lung tissue engineering and hopefully opens up an exciting area of research with great possibilities.

Appendices

A.1 Pulmonary Surfactant

Pulmonary surfactant plays a very important role for normal lung function. The main function of pulmonary surfactant is to lower the surface tension in the lung. It is a major reason for the hysteresis in the lung pressure-volume curve. In the lung, surfactant reduces the surface tension from 70dynes/cm (surface tension of water) to 0-25 dynes/cm. By decreasing surface tension, the driving forces for instability are greatly diminished during deflation. During inflation however, the surface tension rises from 0 to 25dynes/cm explaining the hysteresis and the shape of the inflation curve. Other functions of surfactant are to reduce the load on the respiratory muscles, improve stability, and "waterproof" the alveoli. The size and shape of the alveoli make them inherently unstable to interfacial surface forces since air seeks out the largest radius of curvature. According to Laplace's Law ($\Delta P = 2\sigma/a$), as the size of the alveoli get bigger (a increases), the decrease in pressure would increase the disequilibrium so that the lung would always be at a highly non-uniform equilibrium state. In normal lungs, four major mechanisms allow the lungs to inflate uniformly and overcome the intrinsic tendency of surface forces to drive the lung to instability and highly non-uniform states of inflation. These are geometry, tissue forces, surfactant, and elastic interdependence.

Pulmonary surfactant is primarily produced by the type II alveolar cells. Surfactant is secreted as lamellar bodies that reorganize into tubular myelin. Tubular myelin releases surfactant which includes primarily lipids (90-95% of surfactant), as well as palmitic acid, fatty acid, and proteins (5-10%). The lipids are primarily dipalmitoyl phosphatidyl choline (DPPC) with 7% phosphatidyl glycerol. There are four types of proteins known so far that are found in surfactant: SP-A, SP-B, SP-C, SP-D. SP-A is a 28-36kDa protein and augments biophysical function with SP-B and is calcium dependent. SP-B is much smaller, 9kDA, and preferentially located in the corners of tubular myelin and increases the adsorption of phospholipids by 100 times. SP-C is also a small protein (4kDa) and interacts with SP-B and plays a backup role. Finally, SP-D plays an immunological role beyond the scope of this project. The proteins in the

surfactant serve to help dispersion and adsorption of the surface components and determine the structure of the tubular myelin.

Surfactant insufficiency increases surface tension and thereby increases the critical opening pressures of the alveoli units. In Respiratory Distress Syndrome of neonates, lungs are highly nonuniform and difficult to recruit. In fact, the pressures required for lung inflation may be too high causing barotraumas to higher compliance regions. Surfactant lowers surface tension and increases surface pressure. The work needed to create a new surface would be low if surface pressure is high. The current view of surfactant function is that at end-expiration, the DPPC monolayer is in a highly compressed solid phase with high surface pressure and low surface tension making energetics favorable towards creating a new surface. At early-inspiration, the solid monolayer breaks apart and fractures into condensed "ice flows" of DPPC monolayers between newly created surfaces lowering the surface pressure and increasing surface tension. At mid-inspiration, the poorly soluble DPPC rapidly adsorbs to the new surface. This surface has poor surface pressure and high surface tension due to the formation of chunks and a multi-layered structure rather than a complete monolayer.

A.2 Protocol

I. Materials
- 3 Sprague Dawley Timed-Pregnant Rat
  i. Average 12 fetuses / mother
  ii. 19-20 days gestation (term = 22 days)
- DHT matrices 8mm in diameter, stored in sterile water until ready for use
- Gelfoam (Pharmacia & Upjohn) gelatin sponges cut 10mm in diameter and stored at 4°C in HBSS until ready for use.
- 4 Agarose-coated 12-well tissue culture plates
- CO_2 gas for asphyxiation or dry ice
- Sterile Gloves – 3 for mother, 3 for fetuses
- 70% ethanol
- 3 autoclaved razor blade (1/mother)
- Forceps for microdissection – 1 straight for mother, 2 straight, 1 angled for fetuses, 4 total – autoclaved
- Scissors for dissection – 1 for mother
- Paper towels
- Disposable bags
- Alcohol swipes to wipe forceps between dissection
- Hank's balanced salt solution - warmed – 2 bottles
- Serum-free F12K media with antibiotics chilled
- Complete F12K media with antibiotics & 10% FBS warmed
- FBS warmed
- Ice bath & Ice tub
- 1000mm-Petri Dishes filled with HBSS – 1 for mother, 1 for fetus
- 100mm- Petri Dishes filled with serum-free media – 1/mother
- 10cc syringes filled with HBSS for lavaging lungs
- 50ml Erlenmeyer BD tubes
- 6 CTC enzyme (1% chicken serum, 0.1% collagenase type I, 0.1% trypsin in Hank's Balanced Salt Solution, filter sterilized and stored frozen -20°C) 30ml/ mother or dozen fetuses
- 6 RNase-free DNase 1000units (1000µl) - Promega
- Styrofoam lid with pins for dissection
- 3 funnels - 2 funnels 41µm nylon mesh, 1 funnel 25µm mesh

II. Dissection
1. Sacrifice one mother at a time by CO_2 asphyxiation (approximately 1-2 minutes)
2. Perform a hysterectomy and remove the fetuses from the uterus placing them in a large Petri dish filled with HBSS.
3. Dissect the fetuses free of the placenta and attendant membranes, cut off the umbilical cords, and place fetuses in a clean Petri dish with fresh HBSS.
4. Pin down the fetus on Styrofoam lid, attaching one needle above the throat, one at the lower abdomen, and one needle at each upper arm.

5. Remove skin: using 2 straight forceps, grip skin at throat, pull skin apart, and avoid piercing the chest wall.
6. Remove the rib cage without piercing heart.
7. Inject HBSS into the heart at the right ventricle to flush the lungs. They should enlarge and lighten in color.
8. Remove the heart and set aside for discard.
9. Remove the lungs and place in Petri dish with serum-free F12K media. Try to remove stray structures, especially bronchi.
10. After removing all the lungs of the fetuses, place dish with lungs on ice and repeat with other mothers until all mothers and fetuses are dissected.

II. Tissue Homogenization and Digestion

1. Transfer the lung tissue to a clean Petri dish with chilled serum-free media, leaving behind blood clots.
2. Place samples onto lid of dish, if necessary, remove excess liquid with 1-ml pipetter.
3. With razor blade, chop the tissue finely. If you have not removed the bronchi, you will notice that the chopped tissue is difficult to separate. Continue to chop until the tissue is well homogenized.
4. Add the sample to the tube of 30ml CTC enzyme solution/mother and 1000units of DNase – both prewarmed to 37°C.
5. Incubate the samples at 37°C, shaking for 15minutes at 300rpm.
6. After the incubation, some digestion should be evident. Swirl the tube and let the undigested tissue fragments settle.
7. Carefully draw off the dissociation fluid using 10-ml pipette and filter the solution into a sterile 50ml conical tube using 1 layer of 41μm mesh over funnel.
8. Wash the tissue with 10ml of serum-free F12K media. Swirl the tube and allow the fragments to settle then draw off the fluid and filter it through the 41μm mesh.
9. Add 10ml of complete media w/10% FBS (total volume now 50ml) to inactivate collagenase and trypsin and pipette up and down to mix well. Store the tubes on ice.
10. Add 30ml CTC enzyme solution and 1000units DNase to remaining tissue fragments and incubate samples at 37°C, shaking for 15mins at 300rpm. After the incubation, the tissue should be complete digested – if tissue remains should be connective tissue.
11. Filter the suspension through the 41μm funnel. Wash the tube with 10ml of serum-free F12K media and filter that solution through.
12. Add 10ml of complete media w/10% FBS to inactivate enzymes (total volume now 50ml) – total of 6 tubes – store on ice.
13. Centrifuge the homogenate for 10 minutes at 1500rpm.
14. Vacuum off the supernatant, keeping the cell pellet and resuspend each tube by mild Vortex mixing.
15. Combine the contents of all the tubes into a single 50-ml centrifuge tube by passing the suspension through a 25μm filter unit. Fill the tube to 50ml with chilled complete media and mix well to wash cells.

16. Equally aliquot 25ml cell suspensions to two 50-ml centrifuge tubes and fill each tube to 50ml with chilled complete media.
17. Perform a viable cell count on one of the tubes via trypan exclusion.
18. Add 15µl trypan blue to 15µl cell suspension and perform cell count. While counting, spin down original cell suspension at 1500rpm for 10 minutes.
19. $T_{cells} = N_{Total\ counted}/(N_{squares\ counted}) * 2 * 10^4 * V_{media}$
20. Re-aliquot the cell suspension to $1.0x10^7$viable cells/50ml media
21. Centrifuge the tubes for 6mins at 1500rpm. Draw off and discard supernatant leaving 50 – 100µl of fluid overlaying.
22. Incubate the pellet with a thin layer of supernatant at 37°C for 1 hr. Warm the agarose-coated plates in the incubator at 37°C for 1 hr.
23. Following the incubation period, resuspend the cell pellet in medium to give a final concentration of 10^8 cells/ml determine volume using a 5-ml pipette.
24. Seed cells with a cell-seeding density of $5x10^6$cells/matrix (minimum 1.0 x 10^6 cells/matrix).
25. Determine total volume needed and bring up cells in necessary volume
26. Inoculate each side of matrix with 20µl cell suspension or 20µl complete media for controls.
27. Place in incubator for 10 mins. Then flip matrices and inoculate other side with 20µl cell suspension or 20µl complete media for controls. (0.04ml/scaffold)
28. Incubate for 2-3 hours to allow cells to attach to the substrate, and then add 0.5ml complete media to each well.
29. After 24 hours, add 1.5ml media to each well.
30. After 48 hours, cultures are placed on a rocker platform at a speed of 6 cycles per min.

A.3 Standard Operating Procedure for Pore Characterization using Linear Intercept Method [25]

Image Analysis:

1. Open the image in Scion Image

2. Click on *Threshold* in the **Options** menu. Select 'Options'; 'Threshold'; Slide red region on the palette bar to optimize the selection of matrix struts without selecting pore space. If a lot of background noise becomes black, go to the palette bar on the left and pull down the threshold level until they disappear

3. Click on *Binary* under the **Process** menu. Click on *Make Binary*. The pixels will then be assigned to black or white.

Pore Analysis:

1. Load the "pore characterization macros" by using *Load Macros...* under the **Special** menu. Run *Compute Percentage Area [P]* under the **Special** menu. The % value in the little data window is the black percentage of the area, which can be converted to porosity by subtracting it from 100.

2. Select an area of the image with the oval drawing tool. To get a circle, hold the down the shift key at the same time you are using the oval tool. Try to get as much of the image in the selected area as possible.

3. Setting the Scale
    1. Using a captured scale bar image at the same magnification from which matrix images were captured and *Set Scale* from the **Analyze** menu, calibrate software

    2. First, change the units to micrometers. In the measured distance box enter 1. In the known distance box, enter the average value from the above table multiplied by 10^{-3}. (This last fixes the fact the program reports the distance values multiplied by 10^{3}.)

4. Run *Linear Intercept* under the **Special** menu. This will produce the pore radii at various angles in the selected area. You must do this before you run the next macro. Run *Plot Intercepts* in the **Special** menu. This will plot the pore radii at the various angle and the calculated best-fit ellipse. Another window will give C0, C1, C2.

5. Transfer the C0, C1, and C2 data to an Excel spreadsheet. It is a very long analysis to get to the major and minor axes of the ellipse, but the resulting equations are:

$$a = \frac{1}{\sqrt{C_0 + \sqrt{C_1^2 + C_2^2}}} \qquad (1)$$

$$b = \sqrt{\frac{\sqrt{C_1^2 + C_2^2}}{C_0\sqrt{C_1^2 + C_2^2} + C_2^2 - C_1^2}} \quad (2)$$

$$\text{aspect ratio (AR)} = a/b \quad (3)$$

$$\text{pore diameter} = 3\sqrt{\left(a^2 + b^2/2\right)} \quad (4)$$

The value '3' comes from 2 (converting radius to diameter) multiplied by 1.5 (multiplication factor used to take into account the underestimate of pore diameter due to angle at which pore was sectioned). The majority of pores will not be sectioned along their true cross-section, but rather at an arbitrary angle which would skew their calculated pore size, this multiplication factor corrects this underestimate.

References

1. Reilly, J.J., *Lung Transplantation and Lung Volume Reduction Surgery.* 2004: Cambridge, MA.
2. Arcasoy, S. and R. Kotloff, *Lung Transplantation.* New England Journal of Medicine, 1999. **340**(14): p. 1081-1091.
3. Kotloff, R., *Lung Transplantation.* New England Journal of Medicine, 2004. **350**(11): p. 1161-1162.
4. Cotran, R.S., V. Kumar, and T. Collins, *Robbins Pathologic Basis of Diseases - 6th ed.* 1999: p. 697 - 698.
5. Berne, P., et al., *Physiology.* 5th ed. 2004, St. Louis: Mosby.
6. Fuchs, S., et al., *Models of the alveolar epithelium.*
7. Douglas, W.H., R.A. Redding, and M. Stein, *The Lamellar Substructure of Osmiophilic Inclusion Bodies Present in Rat Type II Alveolar Pneumonocytes.* Tissue & Cell, 1975. **7**(1): p. 137 - 142.
8. Sannes, P.L., *Structural and functional relationships between type II pneumocytes and components of extracellular matrices.* Exp. Lung Res., 1991. **17**(4): p. 639 - 59.
9. Douglas, W.H. and R.W. Teel, *An Organotypic in Vitro Model System for Studying Pulmonary Surfactant Production by Type II Alveolar Pneumonocytes.* American Review of Respiratory Disease, 1976. **113**: p. 17 - 23.
10. Sugihara, H., et al., *Reconstruction of Alveolus-Like Structure from Alveolar Type II Epithelial Cells in Three-Dimensional Collagen Gel Matrix Culture.* American Journal of Pathology, 1993. **142**(3): p. 783 - 92.
11. Batenburg, J.J., et al., *Isolation of alveolar type II cells from fetal rat lung by differential adherence in monolayer culture.* Biochimica et Biophysica Acta, 1988. **960**: p. 441 - 453.
12. Blau, H., et al., *Fetal Type 2 Pneumocytes Form Alveolar-Like Structures and Maintain Long-Term Differentiation on Extracellular Matrix.* Journal of Cellular Physiology, 1988. **136**: p. 203 - 214.
13. Dobbs, L.G., *Isolation and culture of alveolar type II cells.* American Journal of Physiology, 1990. **258**: p. L134 - L147.
14. Douglas, W.H., et al., *Visualization of Cellular Aggregates Cultured on a Three Dimensional Collagen Sponge Matrix.* In Vitro., 1980. **16**(4): p. 306- 312.
15. Adamson, I.Y., G. King, and L. Young, *Influence of Extracellular Matrix and Collagen Components of Alveolar Type 2 Cell Morphology and Function.* In Vitro Cellular & Developmental Biology, 1989. **25**(6): p. 494 - 502.
16. Geppert, E.F., M.C. Williams, and R. Mason, *Primary culture of rat alveolar type II cells on floating collagen membranes. Morphological and biochemical observations.* Exp. Cell Res., 1980. **128**(2): p. 363 - 74.
17. Lwebuga-Mukasa, J.S., D.H. Ingbar, and J.A. Madri, *Repopulation of a Human Alveolar Matrix by Adult Rat Type II Pneumocytes In Vitro.* Experimental Cell Research, 1986. **162**: p. 423 - 435.
18. Shannon, J.M., R. Mason, and S.D. Jennings, *Functional differentiation of alveolar type II epithelial cells in vitro effects of cell shape, cell-matrix*

interactions and cell-cell interactions. Biochimica et Biophysica Acta, 1987. **931**: p. 143 - 156.

19. Douglas, W.H. and P.M. Farrell, *Isolation of Cells that Retain Differentiated Functions in Vitro: Properties of Clonally Isolated Type II Alveolar Pneumonocytes.* Environmental Health Perspectives, 1976. **16**: p. 83 - 88.
20. Douglas, W.H., G.W. Moorman, and R.W. Teel, *The Formation of Histotypic Structures from Monodisperse Fetal Rat Lung Cells Cultured on a Three-Dimensional Substrate.* In Vitro., 1976. **12**(5): p. 373 - 81.
21. Post, M. and B.T. Smith, *Histochemical and Immunocytochemical Identification of Alveolar Type II Epithelial Cells Isolated from Fetal Rat Lung.* Am. Rev. Respir. Dis., 1988. **137**: p. 525 - 530.
22. O'Brien, F., et al., *Influence of freezing rate on pore structure in freeze-dried collagen-GAG scaffolds.* Biomaterials, 2004. **25**: p. 1077-1086.
23. Taconic, *Use of Timed-Pregnant SD Rats in Current Biomedical Research.* Research Animal Review, Fall 1994. **1**.
24. Douglas, W.H., J.A. McAteer, and T. Cavanagh, *Organotypic Culture of Dissociated Fetal Rat Lung Cells on a Collagen Sponge Matrix.* TCA Manual, 1978. **4**(1): p. 749 - 753.
25. O'Brien, F., *Standard Operating Procedure for Pore Characterization using Linear Intercept Method.* 2002.
26. Yannas, I., *Tissue and Organ Regeneration in Adults.* 2001, New York: Springer.
27. Benali, R., et al., *Tubule Formation and Functional Differentiation by Human Epithelial Respiratory Cells Cultured in a Three-Dimensional Collagen Matrix.* Chest., 1992. **101**(3 Suppl): p. 7S - 9S.
28. Sorokin, S., *A study of development in organ cultures of mammalian lungs.* Develop. Biol., 1961. **3**: p. 60 - 83.
29. Mason, R., et al., *Identification of Rat Alveolar Type II Epithelial Cells with a Tannic Acid and Polychrome Stain.* Am. Rev. Respir. Dis., 1985. **131**: p. 786-788.
30. Gaillard, D. and E. Puchelle, *Differentiation and Maturation of Airway Epithelial Cells: Role of Extracellular Matrix and Growth Factors*, in *Lung Development.*